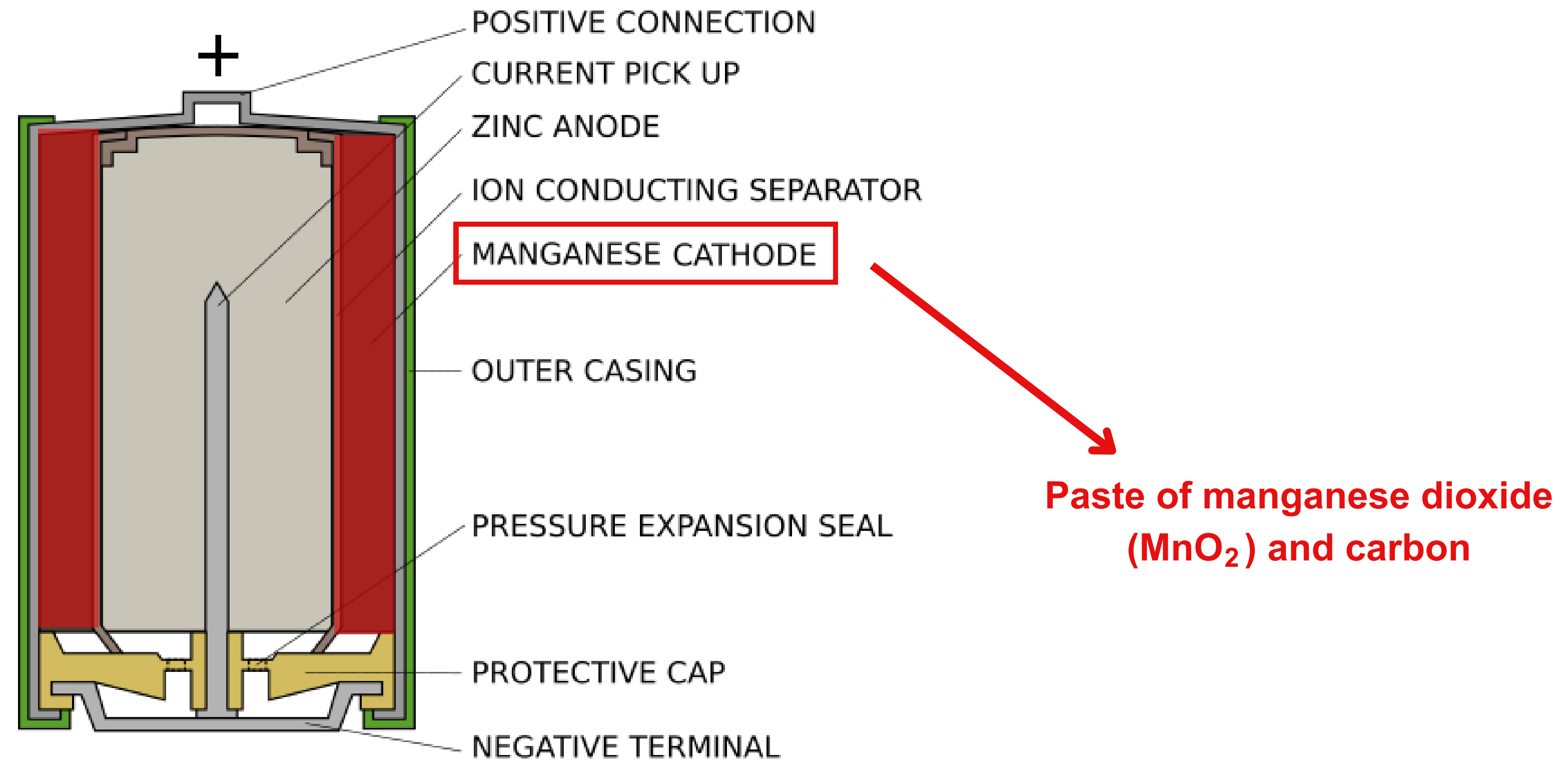




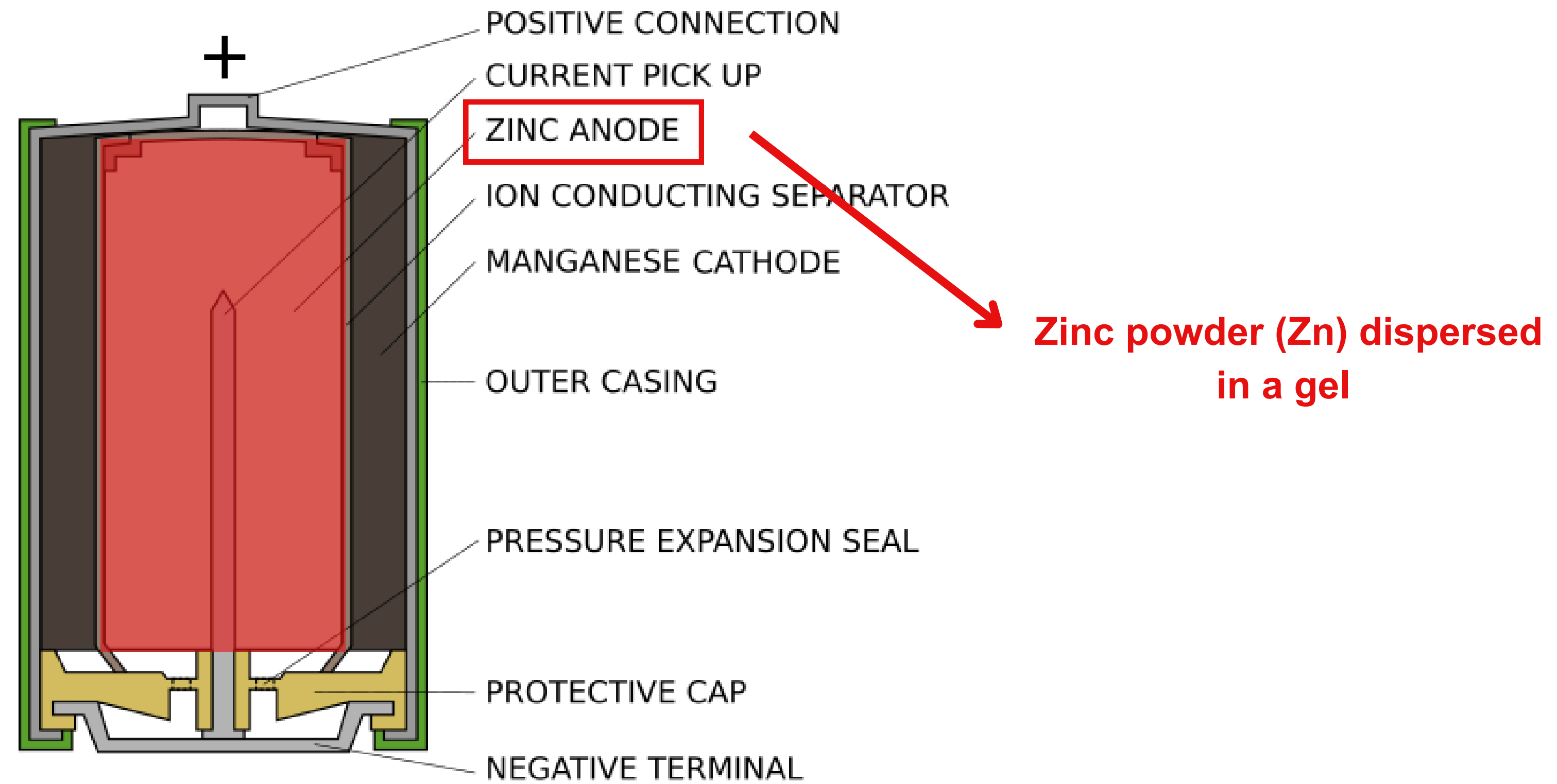
Kinetic Voltmeter

A DIY method of testing the charge of a battery is to drop it on a hard surface and observe whether it bounces. Explain the phenomenon and find other non-invasive mechanical methods to estimate the remaining charge. Optimize the accuracy of your method.

Zinc-Manganese Alkaline Battery

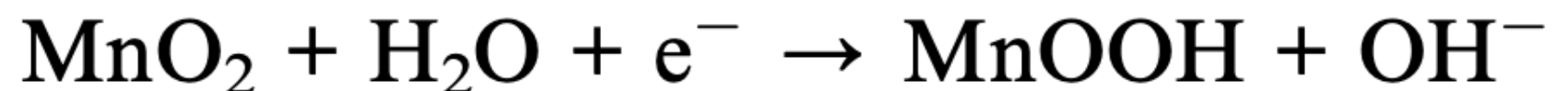


Zinc-Manganese Alkaline Battery



Potential difference and discharge process

RedOx reaction



Potential difference and discharge process

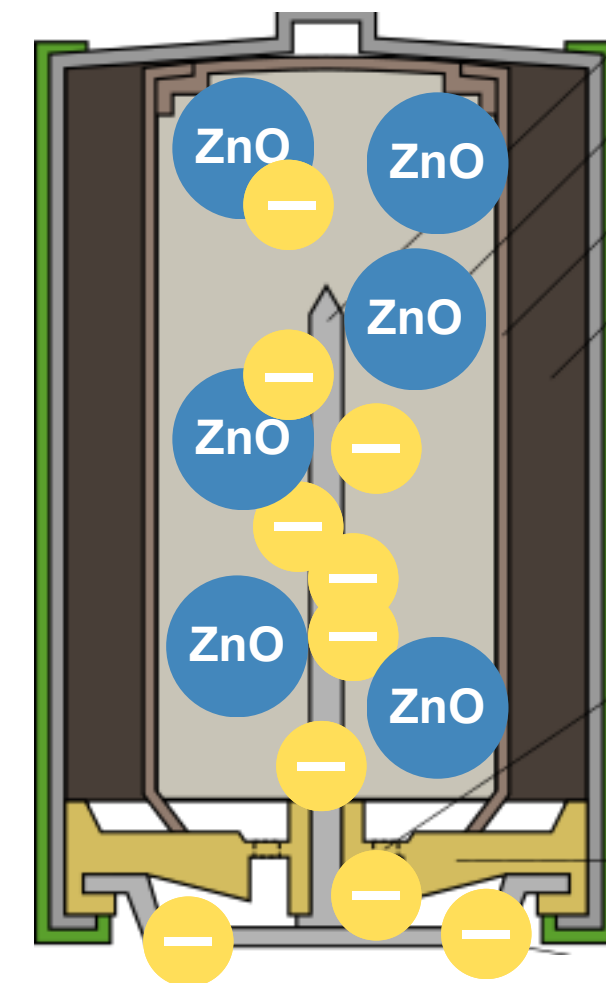
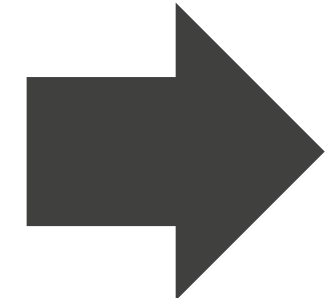
RedOx reaction



Oxidation



Reduction

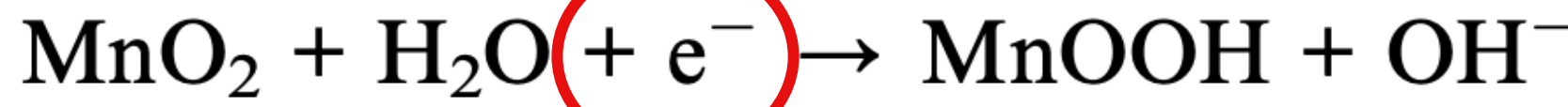


Potential difference and discharge process

RedOx reaction



Oxidation

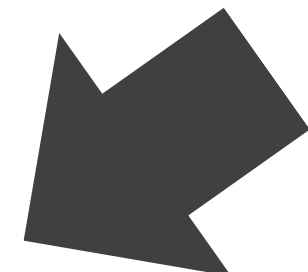
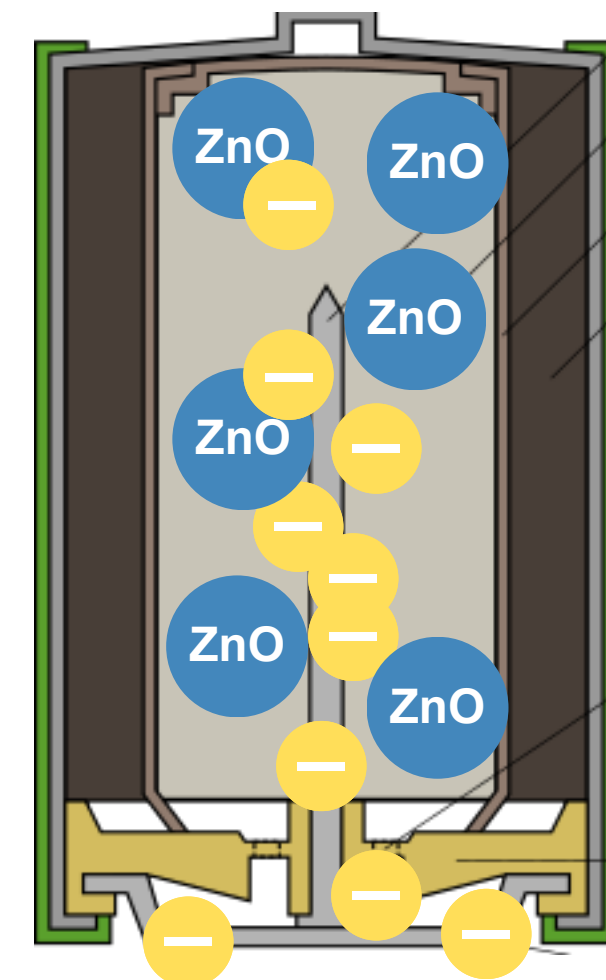


Reduction

Discharged



Charged

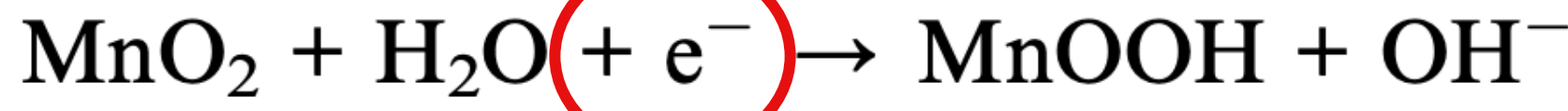


Potential difference and discharge process

RedOx reaction



Oxidation

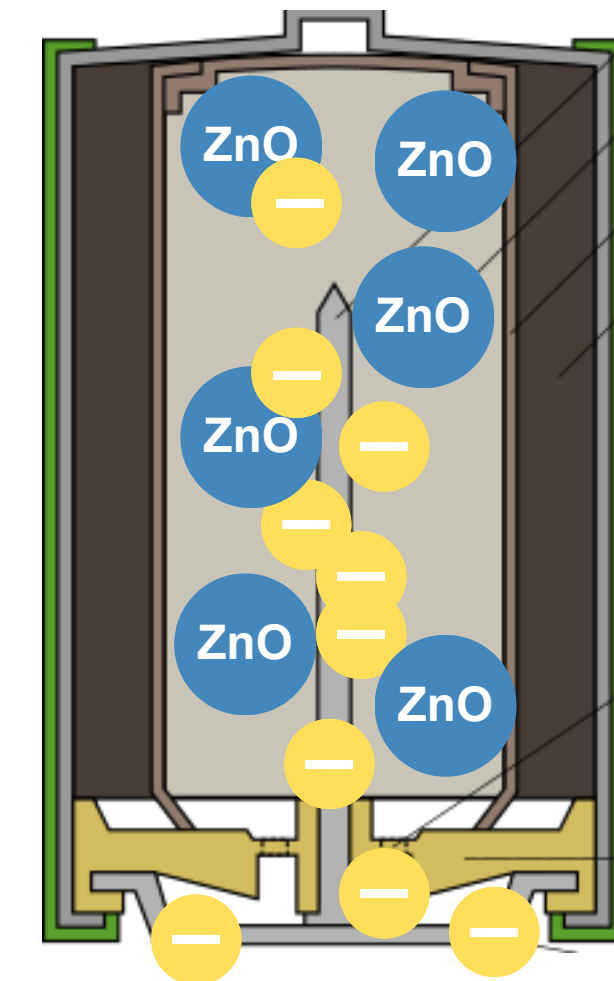
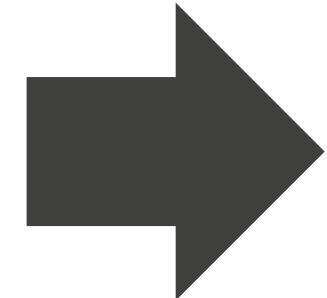


Reduction

Discharged

Battery's Capacity (mAh)

total amount of electrical charge that the battery can deliver



Charged



Current Knowledge

Journal of
Materials Chemistry A



COMMUNICATION

[View Article Online](#)

[View Journal](#) | [View Issue](#)



CrossMark
click for updates

Cite this: *J. Mater. Chem. A*, 2015, 3,
9395

Received 3rd March 2015
Accepted 11th March 2015

DOI: 10.1039/c5ta01576f

www.rsc.org/MaterialsA

The relationship between coefficient of restitution and state of charge of zinc alkaline primary LR6 batteries†

Shoham Bhadra,^a Benjamin J. Hertzberg,^b Andrew G. Hsieh,^b Mark Croft,^c Joshua W. Gallaway,^d Barry J. Van Tassell,^e Mylad Chamoun,^f Can Erdonmez,^f Zhong Zhong,^g Tal Sholklapper^h and Daniel A. Steingart^{*b}

The coefficient of restitution of alkaline batteries has been shown to increase as a function of depth of discharge. In this work, using non-destructive mechanical testing, the change in coefficient of restitution is compared to *in situ* energy-dispersive X-ray diffraction data to determine the cause of the macroscopic change in coefficient of restitution. The increase in coefficient of restitution correlates to the formation of a percolation pathway of ZnO within the anode of the cell, and the coefficient of restitution levels off at a value of 0.66 ± 0.02 at 50% state of charge when the anode has densified into porous ZnO solid. Of note is the sensitivity of coefficient of restitution to the amount of ZnO formation that rivals the sensitivity of *in situ* energy-dispersive X-ray diffraction.

of these methods makes them unfeasible for applications in which the cell must remain intact. Methods such as X-ray diffraction (XRD),¹² X-ray microtomography,^{13–15} and acoustic emission sensing^{16–19} allow for non-destructive *in situ* characterization of the microstructure, but these methods require specialized equipment and, with few exceptions, cannot be applied *in operando*.

Recently there has been popular interest²⁰ in the tendency of an alkaline AA battery to bounce after being dropped on its end when discharged to full capacity, compared to a flat landing with minimal bounce when the battery is “as-received”. In this paper the coefficient of restitution (COR) of an alkaline AA

Complementary studies :

Q. C. Horn and Y. Shao-Horn, *J. Electrochem. Soc.*, 2003, **150**, A652–A658.

I. Arise, S. Kawai, Y. Fukunaka and F. R. McLarnon, *J. Electrochem. Soc.*, 2013, **160**, D66–D74.

Current Knowledge

Journal of
Materials Chemistry A



COMMUNICATION

[View Article Online](#)

[View Journal](#) | [View Issue](#)



CrossMark
click for updates

Cite this: *J. Mater. Chem. A*, 2015, 3,
9395

Received 3rd March 2015
Accepted 11th March 2015

DOI: 10.1039/c5ta01576f

www.rsc.org/MaterialsA

The relationship between coefficient of restitution and state of charge of zinc alkaline primary LR6 batteries†

Shoham Bhadra,^a Benjamin J. Hertzberg,^b Andrew G. Hsieh,^b Mark Croft,^c Joshua W. Gallaway,^d Barry J. Van Tassell,^e Mylad Chamoun,^f Can Erdonmez,^f Zhong Zhong,^g Tal Shoklapper^h and Daniel A. Steingart^{*b}

The coefficient of restitution of alkaline batteries has been shown to increase as a function of depth of discharge. In this work, using non-destructive mechanical testing, the change in coefficient of restitution is compared to *in situ* energy-dispersive X-ray diffraction data to determine the cause of the macroscopic change in coefficient of restitution. The increase in coefficient of restitution correlates to the formation of a percolation pathway of ZnO within the anode of the cell, and the coefficient of restitution levels off at a value of 0.66 ± 0.02 at 50% state of charge when the anode has densified into porous ZnO solid. Of note is the sensitivity of coefficient of restitution to the amount of ZnO formation that rivals the sensitivity of *in situ* energy-dispersive X-ray diffraction.

of these methods makes them unfeasible for applications in which the cell must remain intact. Methods such as X-ray diffraction (XRD),¹² X-ray microtomography,^{13–15} and acoustic emission sensing^{16–19} allow for non-destructive *in situ* characterization of the microstructure, but these methods require specialized equipment and, with few exceptions, cannot be applied *in operando*.

Recently there has been popular interest²⁰ in the tendency of an alkaline AA battery to bounce after being dropped on its end when discharged to full capacity, compared to a flat landing with minimal bounce when the battery is “as-received”. In this paper the coefficient of restitution (COR) of an alkaline AA

Restitution Coefficient (COR)

Ratio of the velocity before and after a collision. In the study, from Newton's law :

$$\text{COR} = \frac{1}{N} \sum_{n=1}^N \sqrt{\frac{h_{n+1}}{h_n}}$$

, n number of bounce

Synthesis of the Study

Experimental techniques

1. Mass measurement (Invariant)

Synthesis of the Study

Experimental techniques

1. Mass measurement (Invariant)
2. Microscopic internal pictures (Post Mortem)

Anode densification into
porous ZnO solid

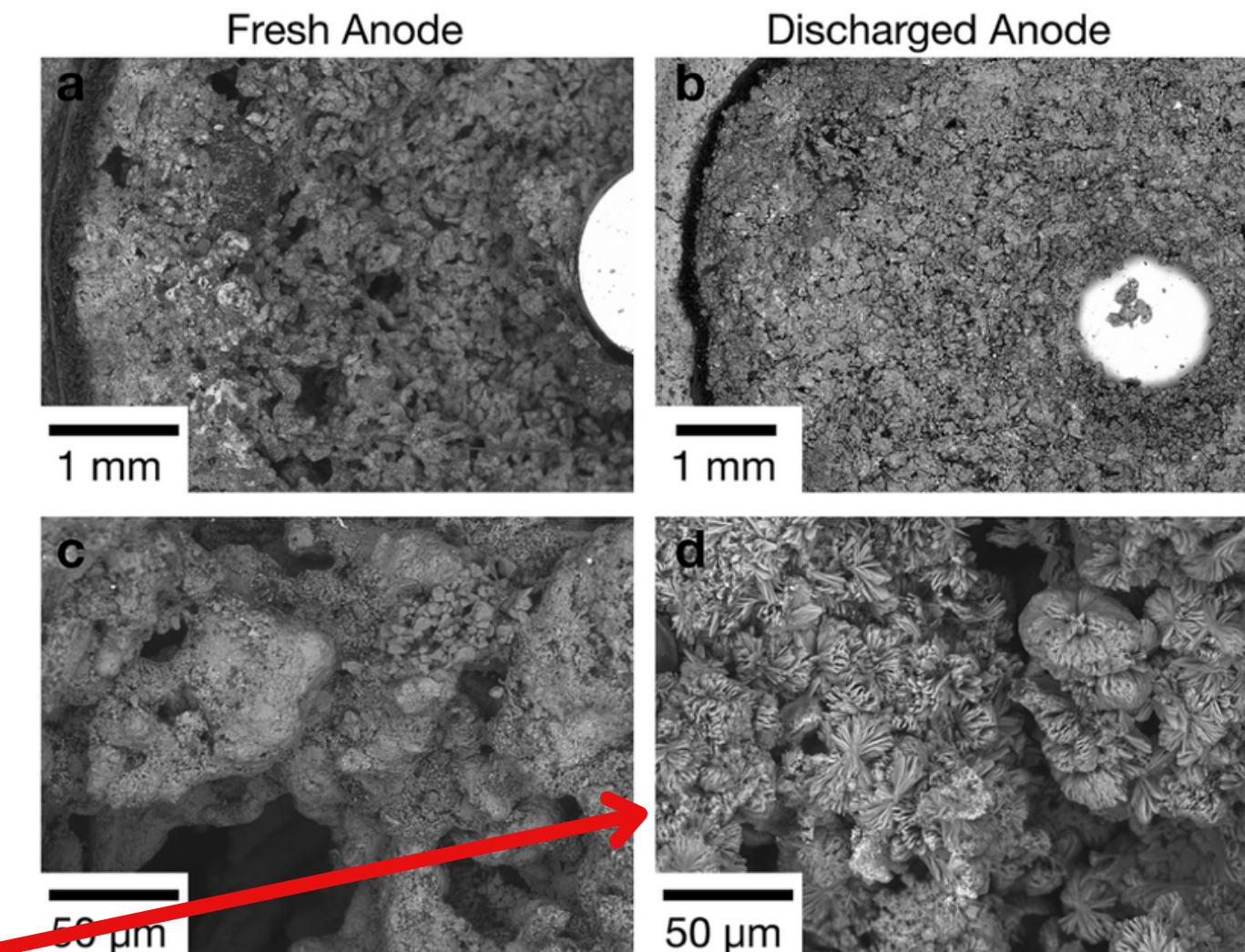


Fig. 1 (a) SEM image of “fresh” cell, where the coarse zinc gel can be seen surrounding the current collector. (b) SEM image of the same cell after full discharge (2850 mA h passed), the anode now largely converted to ZnO. A more compact morphology is seen closest to the separator, with more granular morphology near the pin. (c) High mag. SEM image showing fresh Zn particles. (d) High mag. SEM image showing coagulated ZnO particles after full discharge.

Synthesis of the Study

Experimental techniques

1. Mass measurement (Invariant)
2. Microscopic internal pictures (Post Mortem)
3. Energy-dispersive X-ray diffraction (Material characterization)

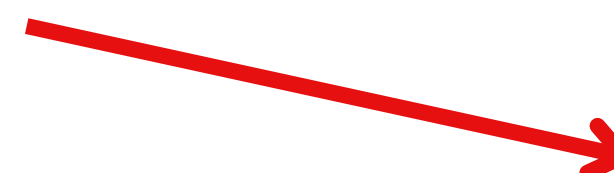
Synthesis of the Study

Experimental techniques

1. Mass measurement (Invariant)
2. Microscopic internal pictures (Post Mortem)
3. Energy-dispersive X-ray diffraction (Material characterization)
4. Mechanical properties of material comparison (Bulk modulus)

Table 3 Materials properties

Increase Bulk Modulus



Material	Density (g cm^{-3}) ²⁹	Bulk Modulus (GPa)
Zinc (Zn)	7.05	59 (ref. 30)
Zinc oxide (ZnO)	5.06	134 (ref. 31)
Ramsdellite (MnO_2)	4.37	119 (ref. 32)
Groutite (MnOOH)	4.14	96 (ref. 33)

Synthesis of the Study – Conclusions

→ Rise in the restitution coefficient is directly linked to the structural evolution of the anode during discharge

Synthesis of the Study – Conclusions

→ **Rise in the restitution coefficient is directly linked to the structural evolution of the anode during discharge**

Explanation :

1. Zinc Oxidation produces a porous zinc-oxide network that densifies the anode, **converting the gel into a rigid solid and restricting the mobility of zinc particles** (and dissipation of kinetic energy)

Synthesis of the Study – Conclusions

→ Rise in the restitution coefficient is directly linked to the structural evolution of the anode during discharge

Explanation :

- Free Zinc particules**
- 1. Zinc Oxidation produces a porous zinc-oxide network that densifies the anode, **converting the gel into a rigid solid and restricting the mobility of zinc particles** (and dissipation of kinetic energy)
- 2. Resulting percolation pathways of zinc oxide facilitate **more efficient transmission of pressure waves** through the cell

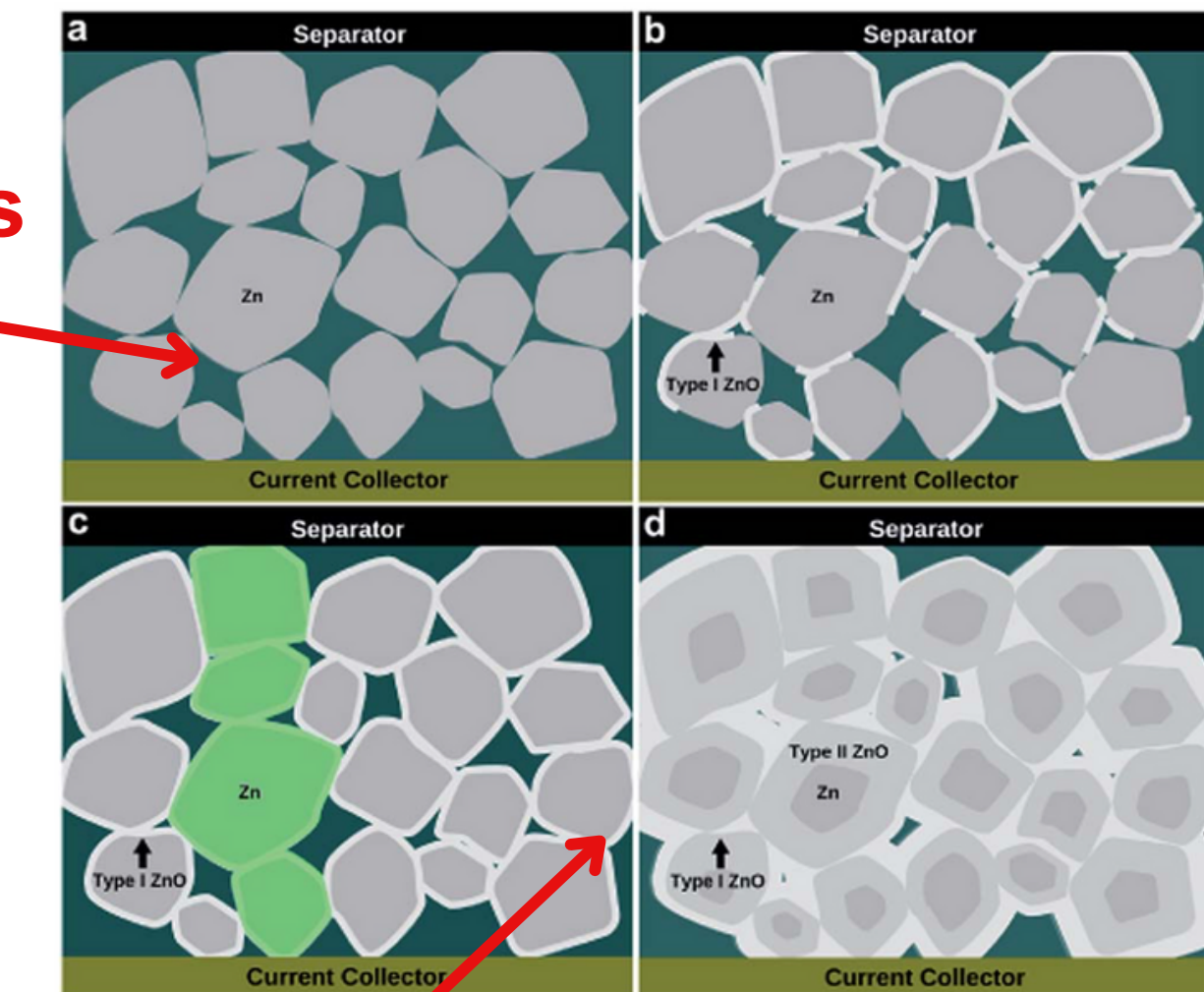


Fig. 4 The progression of ZnO formation in the anode. (a) The initial anode gel comprised of Zn particles in an electrolyte/cellulose matrix. (b) Formation of Type I ZnO shells on Zn particles. Oxidation occurs preferentially at the separator. (c) Formation of a percolation pathway. As all particles become clad in ZnO shells, a contiguous network of ZnO-clad particles forms from separator to current collector (highlighted in green). (d) Densification of the anode. Type I ZnO shells grow and Zn particles oxidize to Type II ZnO.

Percolation pathway and densification

Our own Experiment – setup

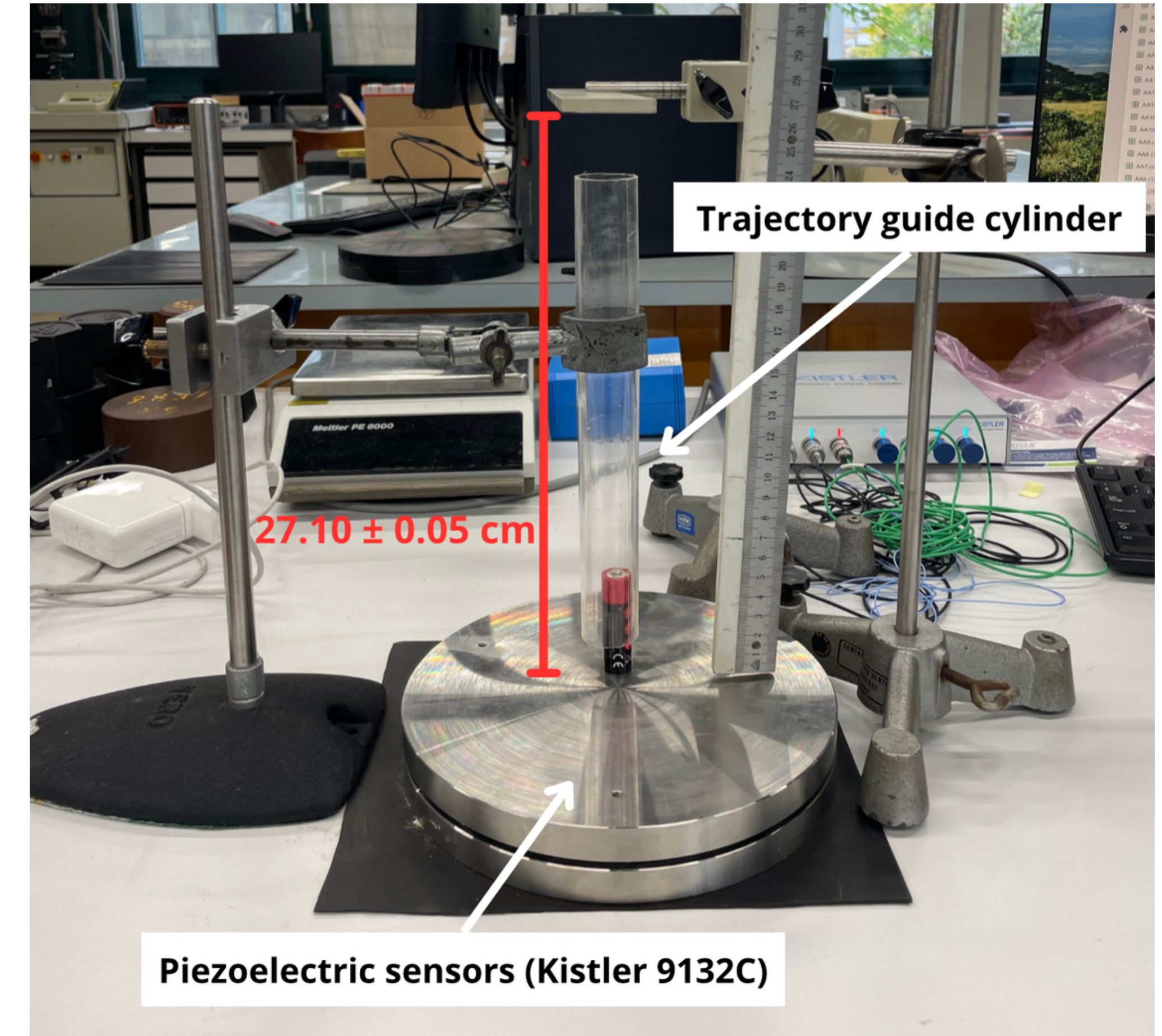
OBI Alkaline LR06 AA



Maximal Tension : 1.5 V

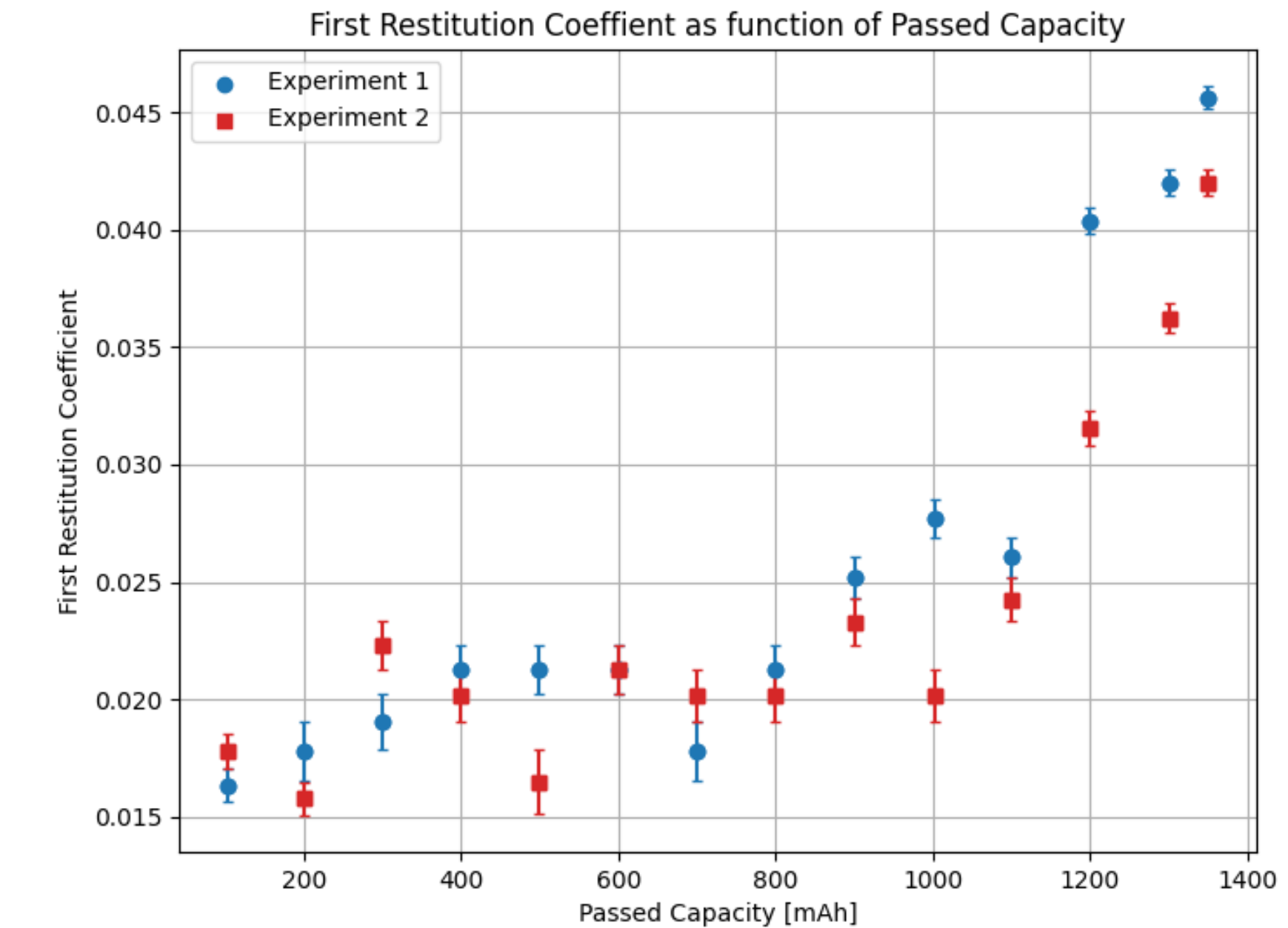
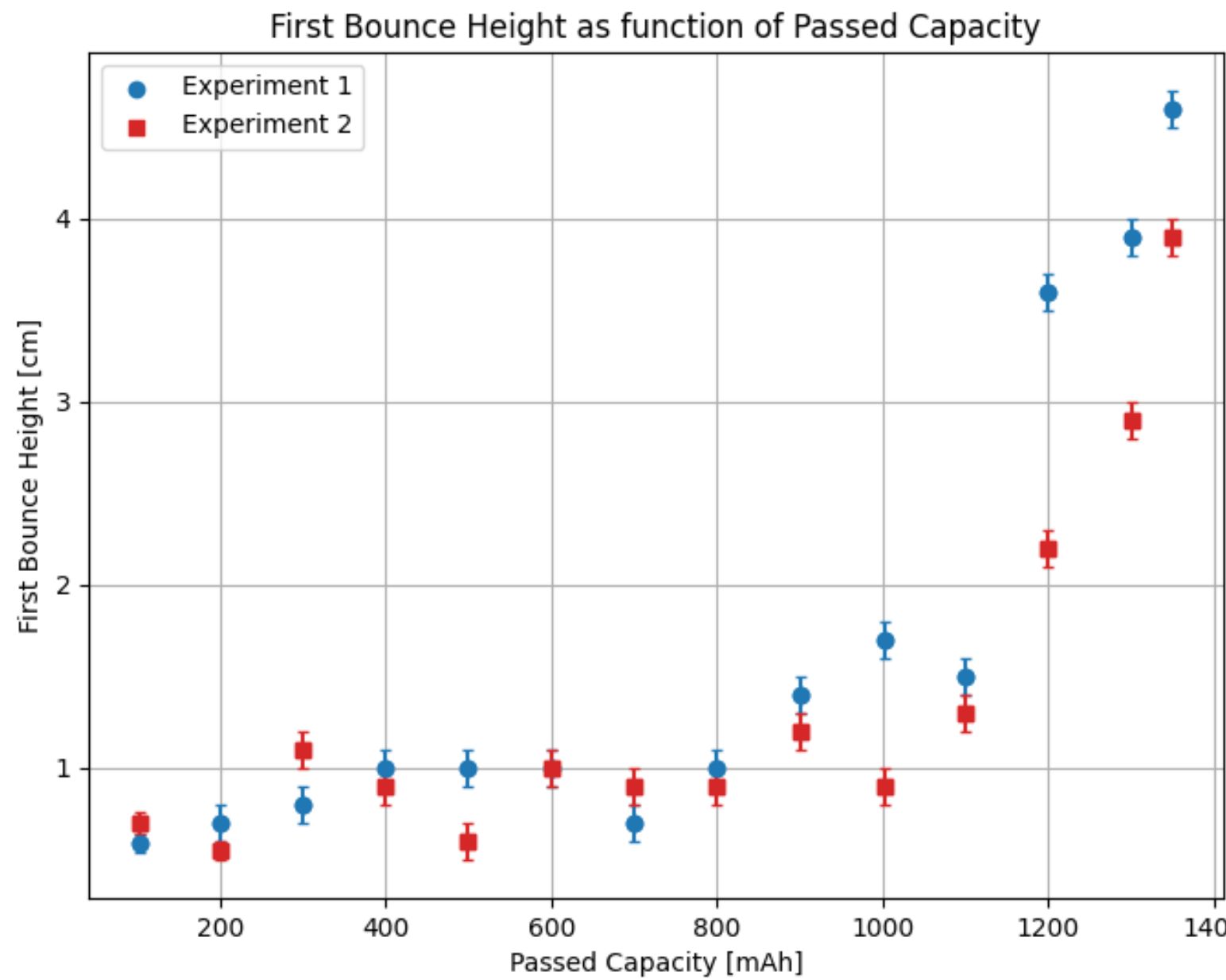
Mass : 23.05 ± 0.03 g

Discharge current : 0.5 A



Our own Experiment – Results

Measure of the bouncing phenomenon

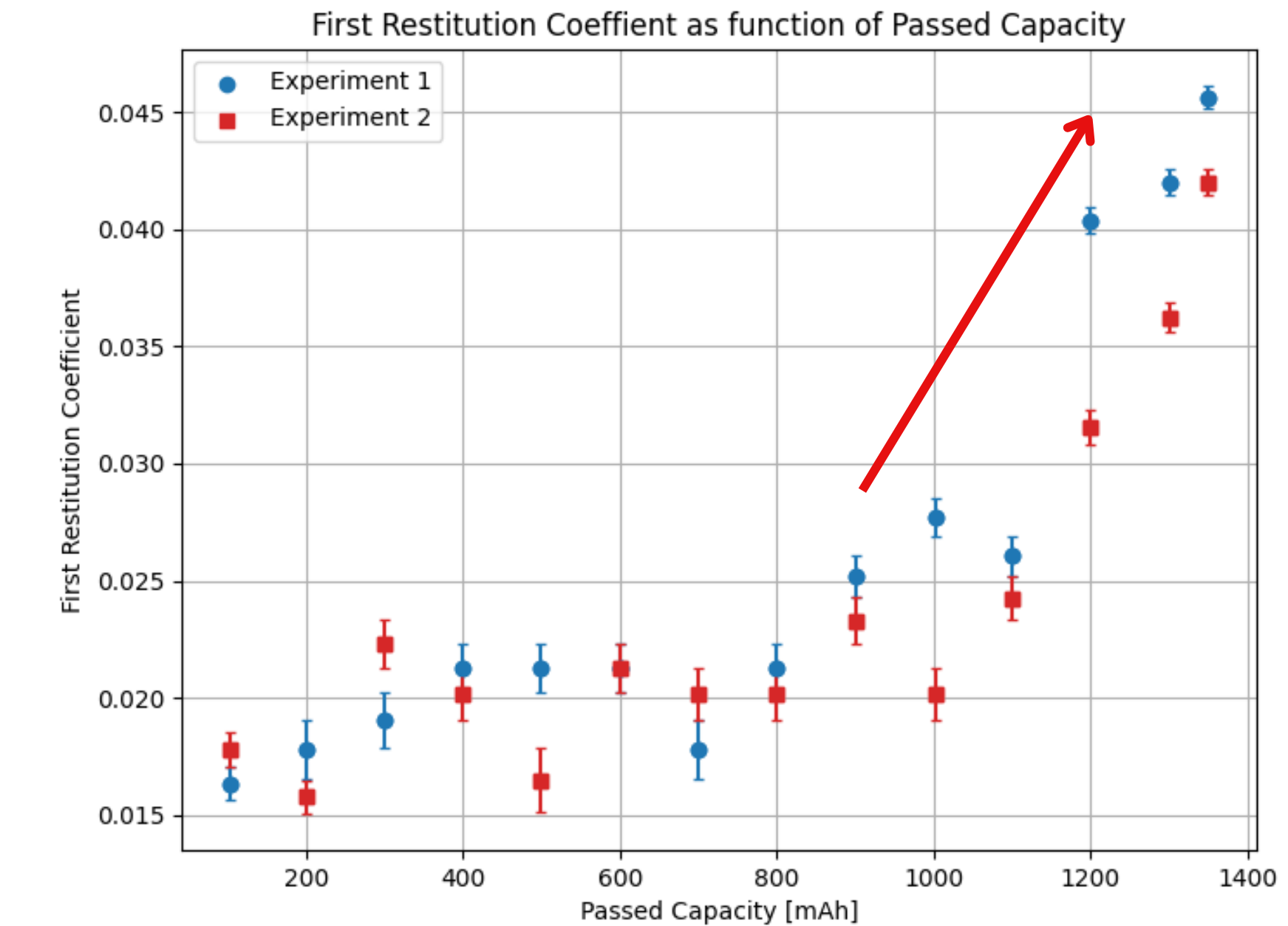
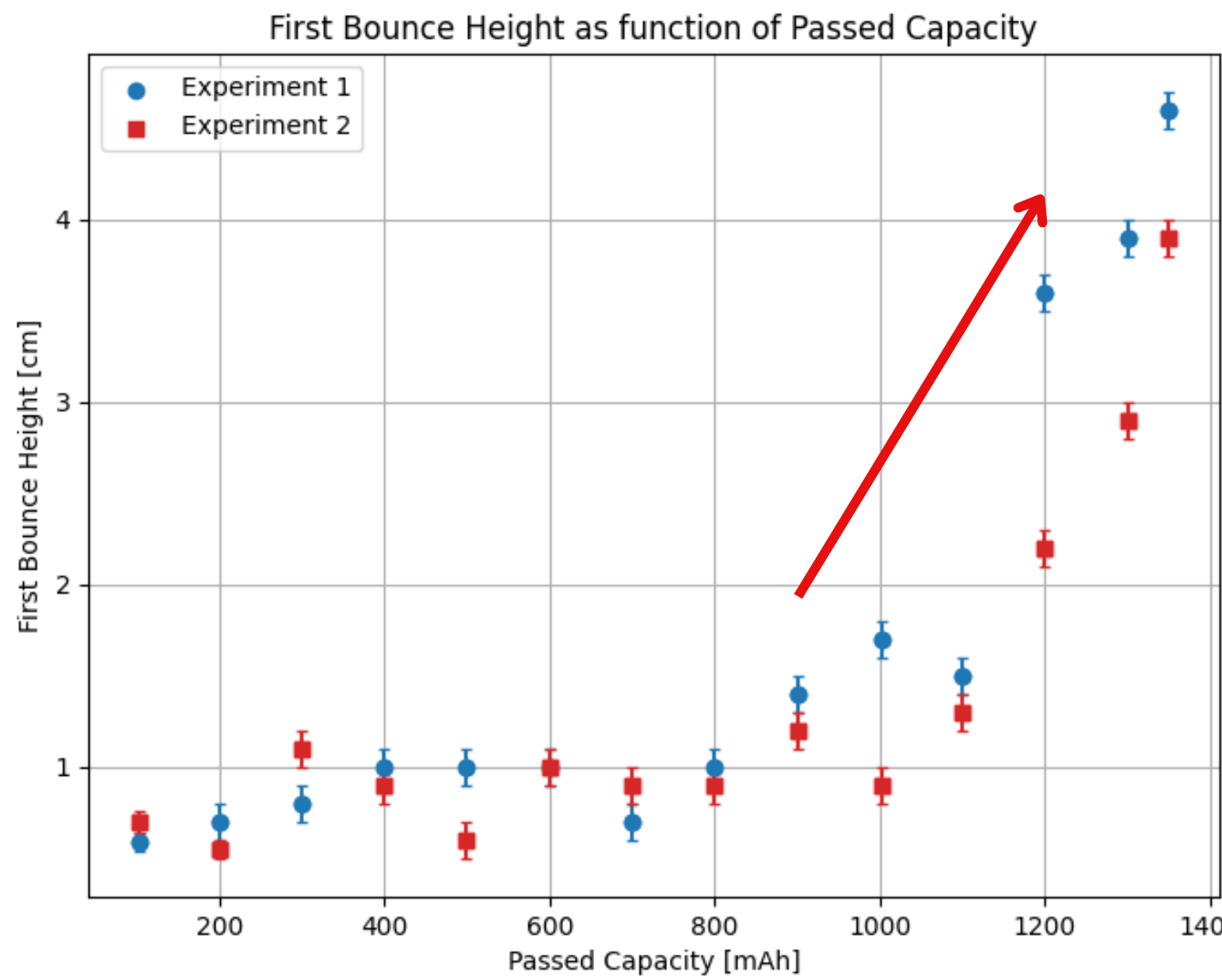


$$h_1 = \frac{1}{2}g\left(\frac{\Delta t_1}{2}\right)^2, \quad \Delta t_1 \text{ time of first bounce}$$

$$\text{COR}_1 = \sqrt{\frac{h_1}{h_0}}$$

Our own Experiment – Results

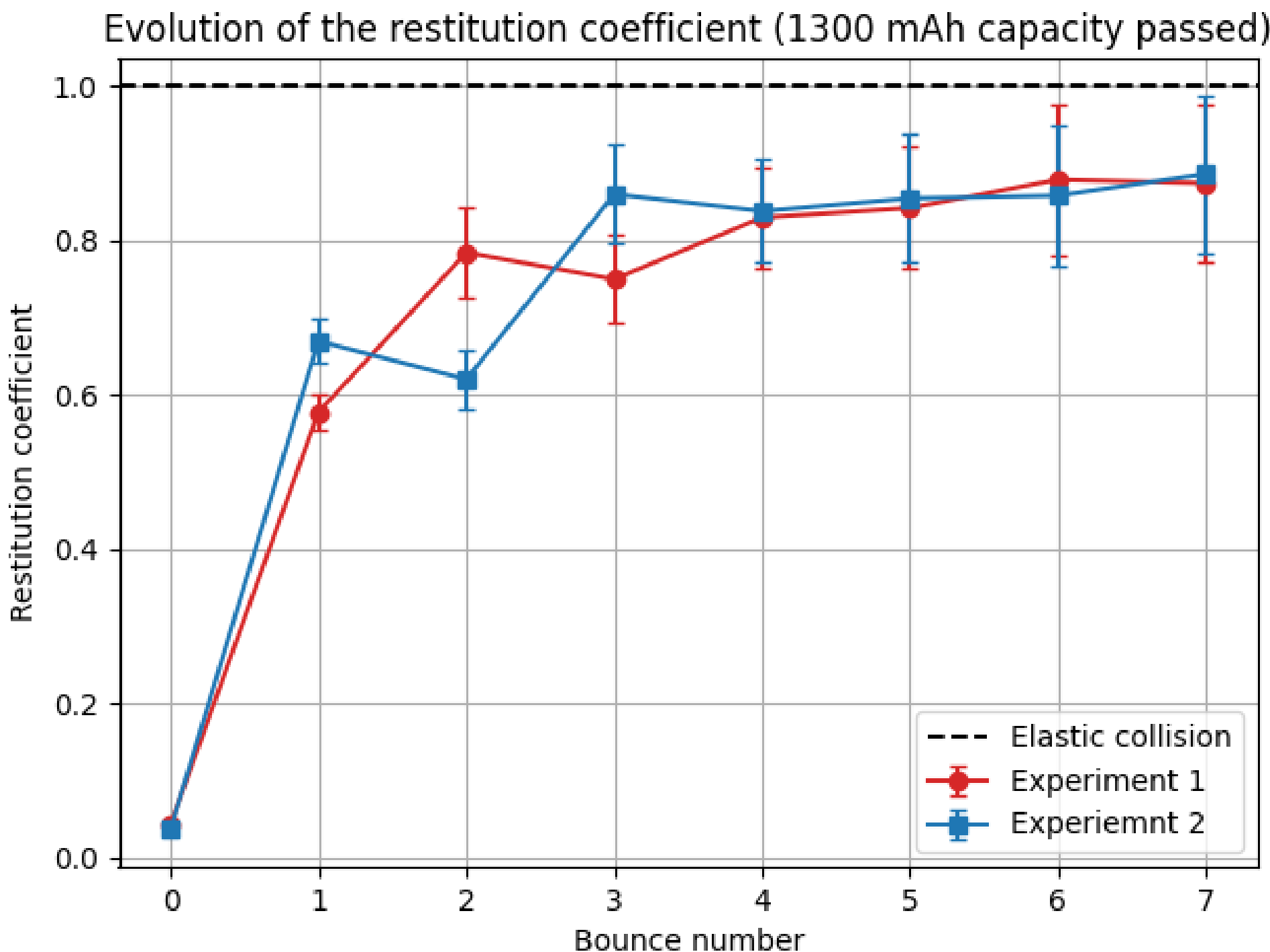
Measure of the bouncing phenomenon



Increase of the bouncing property around 900 mAh passed Capacity

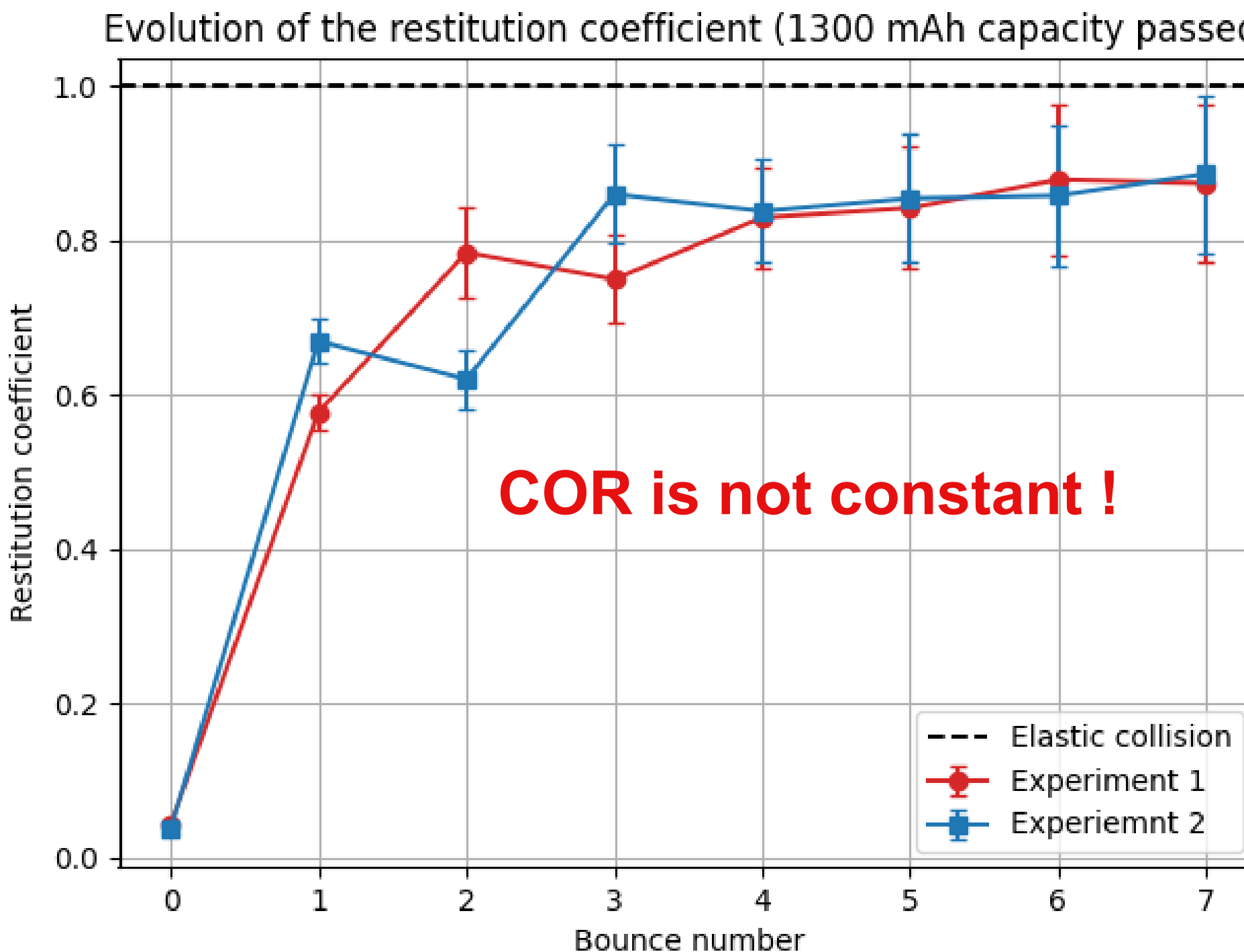
Our own Experiment – Results

What was unexpected



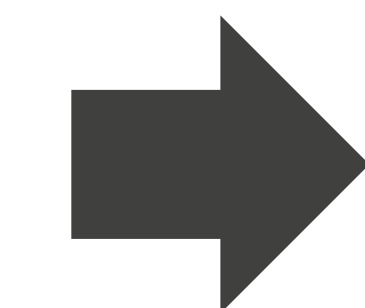
Our own Experiment – Results

What was unexpected



$$\text{COR} = \frac{1}{N} \sum_{n=1}^N \sqrt{\frac{h_{n+1}}{h_n}} = \frac{1}{N} \sum_{n=1}^N e_n = \bar{e}$$

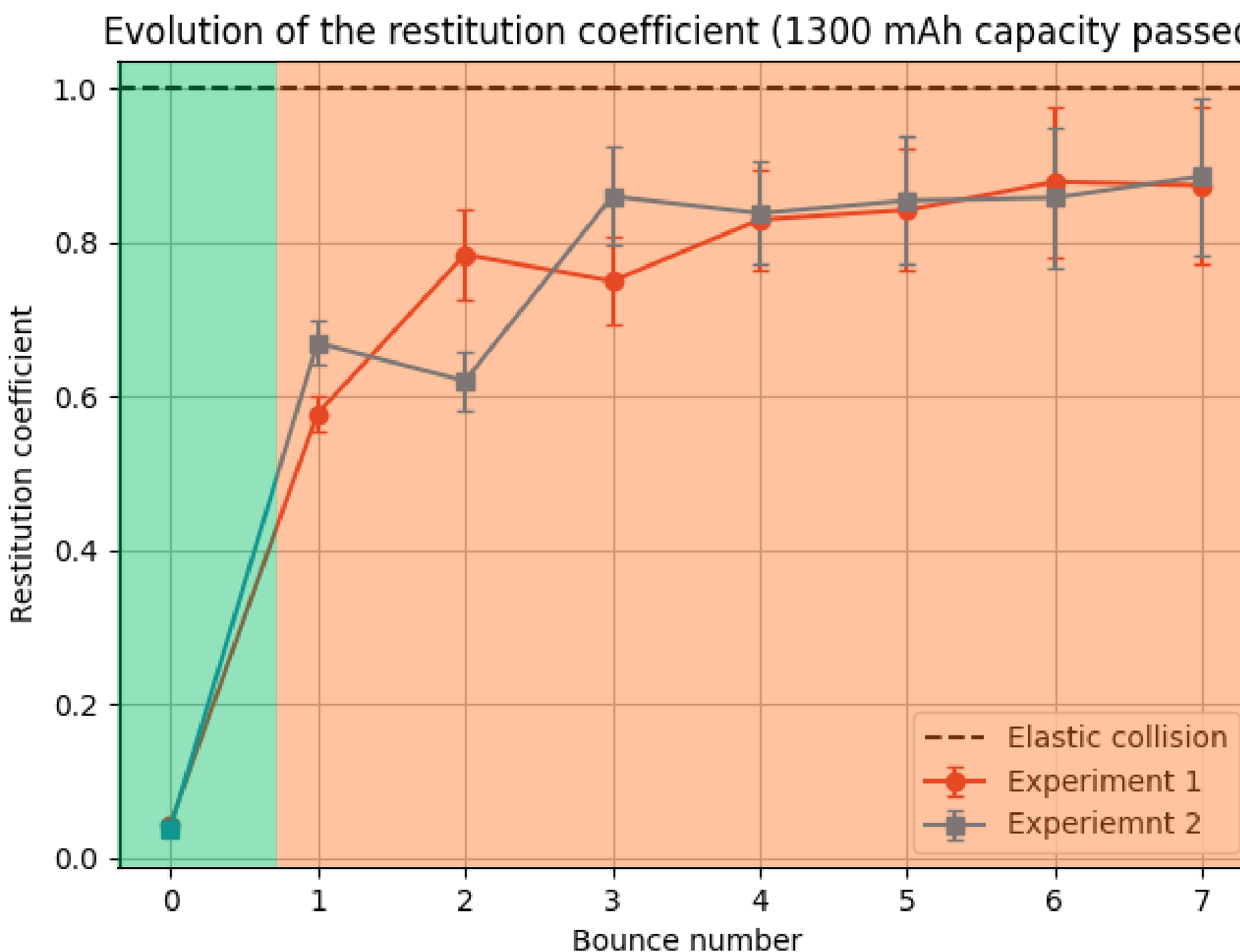
→ No physical significance



Each collision gets **more elastic**,
which means **the smaller the
rebound the more the energy
is restituted**

Our own Experiment – Results

What was unexpected



Observation :

At **low energies**, the **damping** is **less pronounced**, making the **phenomenon more difficult to measure** in this range.

Hypothesis :

Can be explained by the **power being insufficient** for significant **energy dissipation through the displacement of zinc molecules**.

Other non-invasive methods - the piezo method

The piezo



- Potential difference to deformation and vice versa
- $V \propto \delta_{\text{piezo}}$

receptor piezo

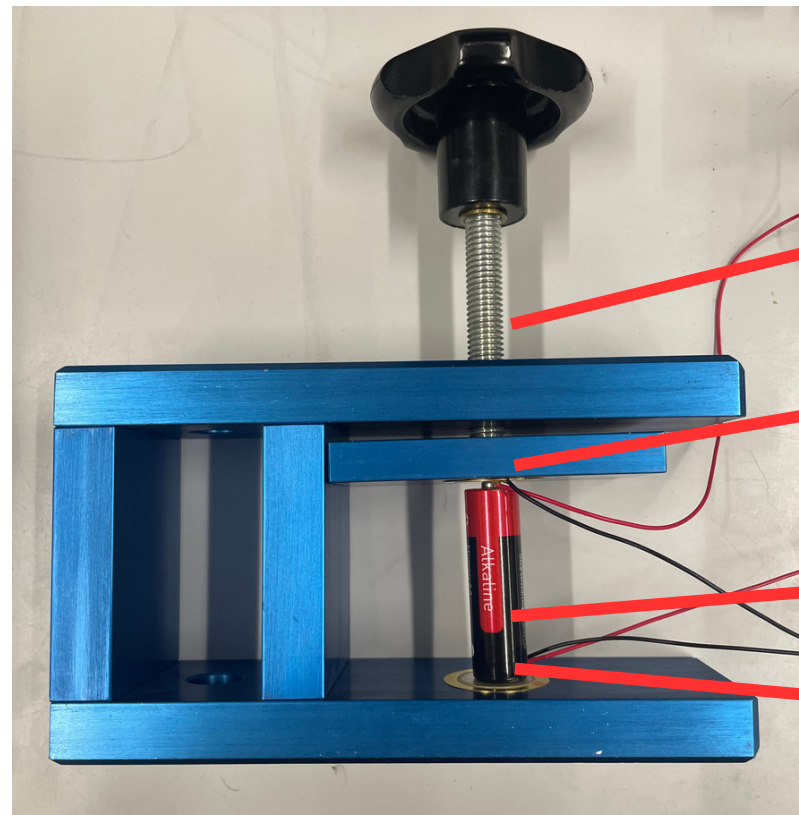


emitter piezo

The idea :

- Discharging implies density change + dampening
 - Different wave behaviours for different SoC
- Emit a wave at one end of the battery, measure the transmitted one at the other end

The piezo method – setup



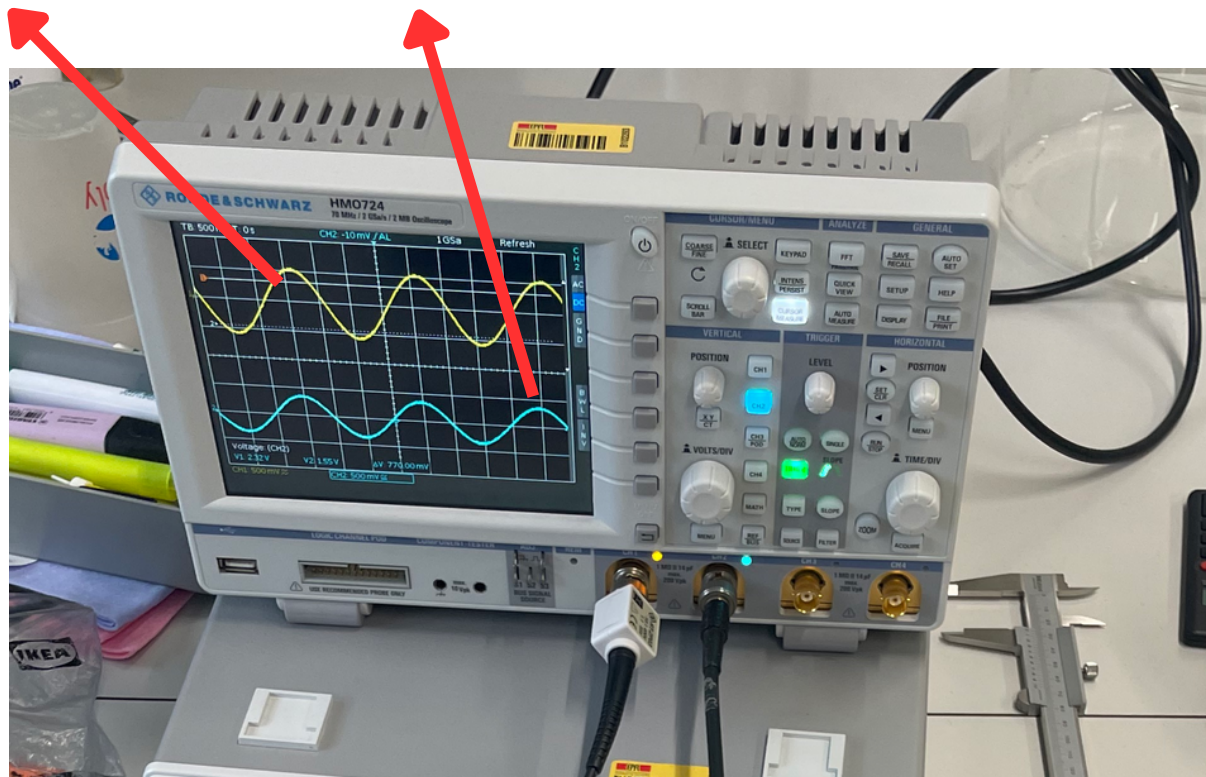
tightening mechanism

receptor piezo

battery

emitter piezo

emitted received



Proper, same frequency sine waves

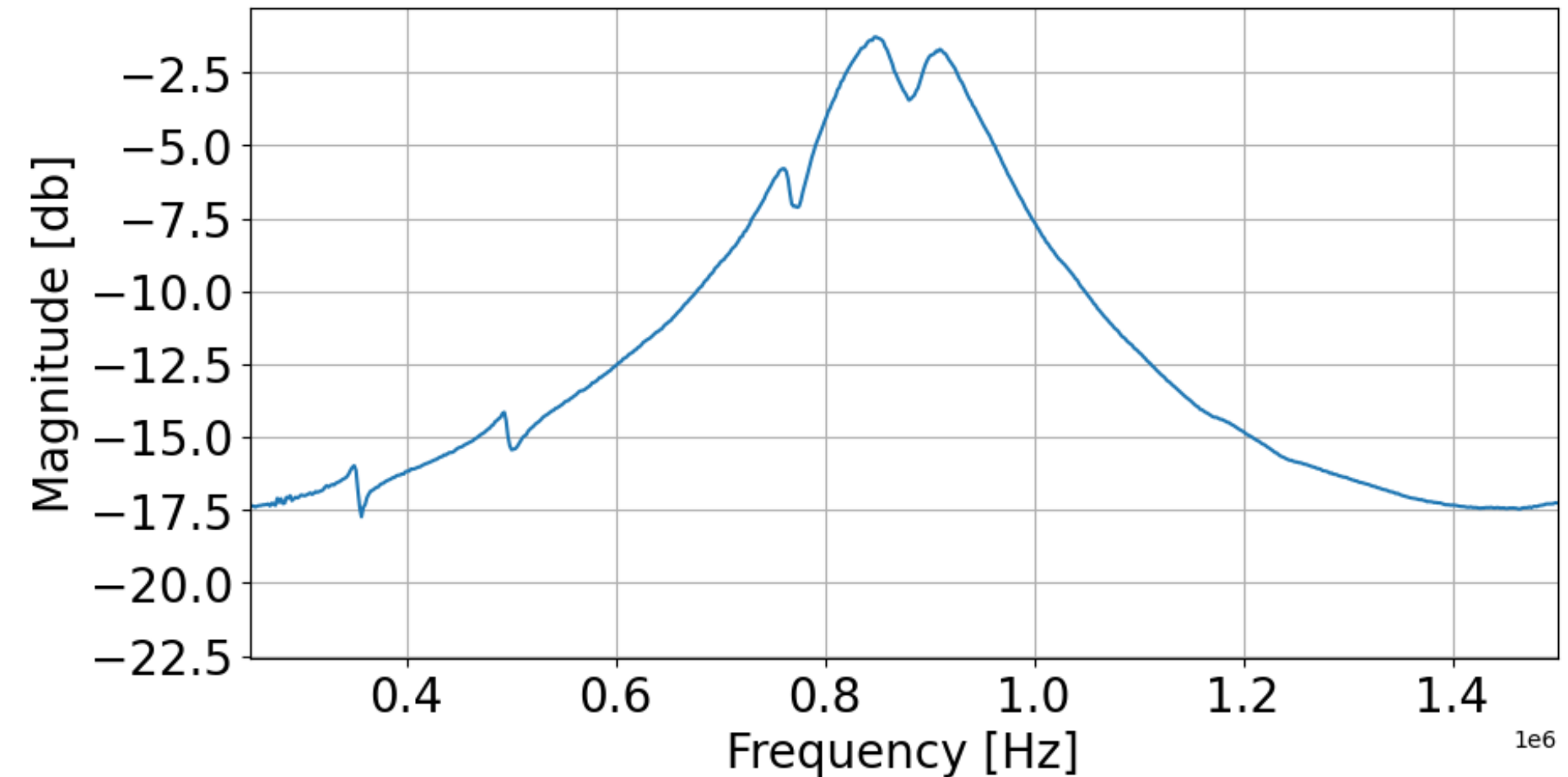
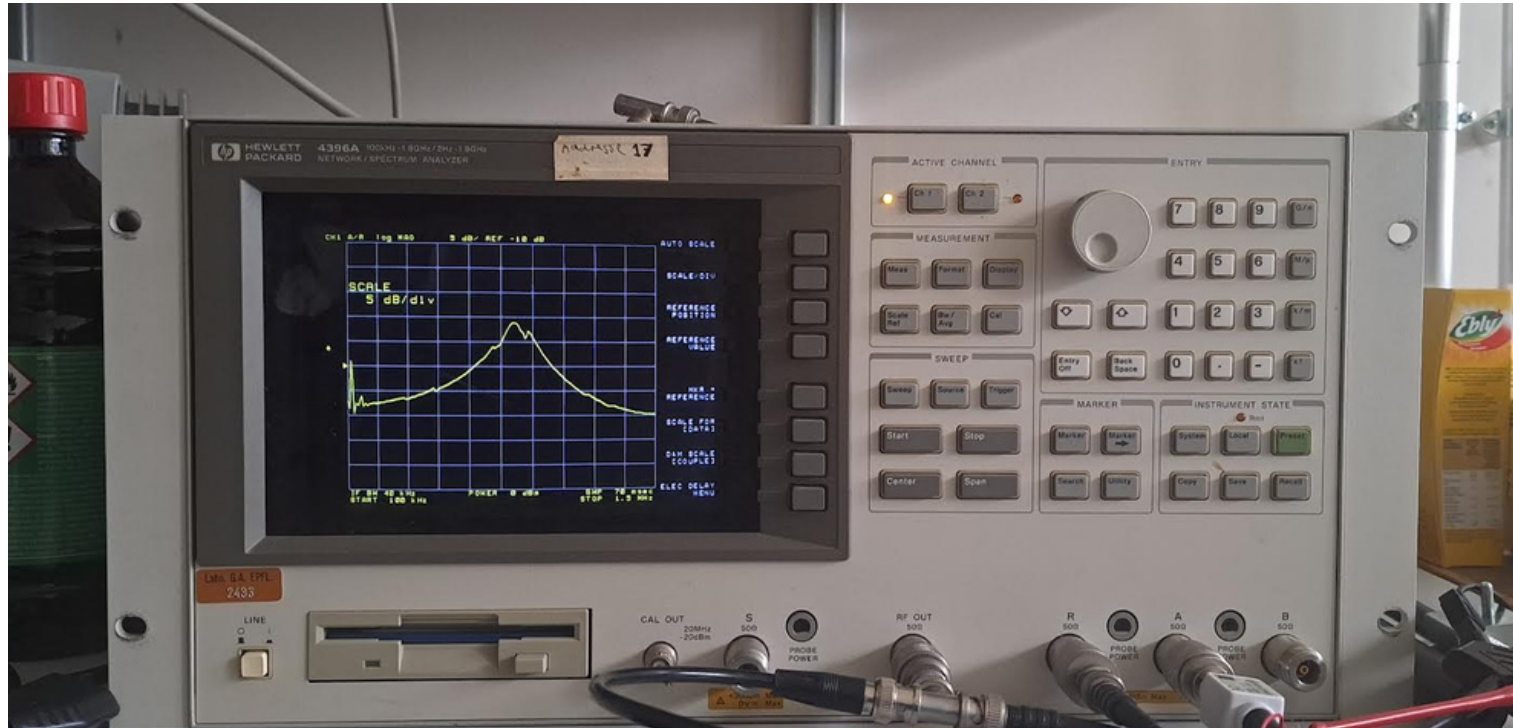
→ local elasticity at the very least, so
wave analysis is relevant

For different amplitudes and frequencies

- gain

The piezo method – results

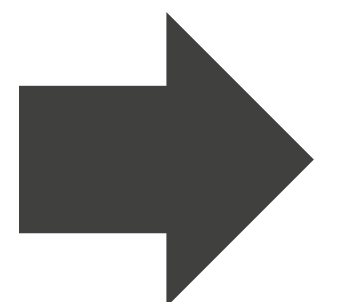
Spectrum analyser to reliably trace the gain curves



Careful : It is a mechanical coupling
Behaves like a forced oscillator

$$m\ddot{x}(t) + c\dot{x}(t) + kx(t) = F_0 \sin(\omega t)$$

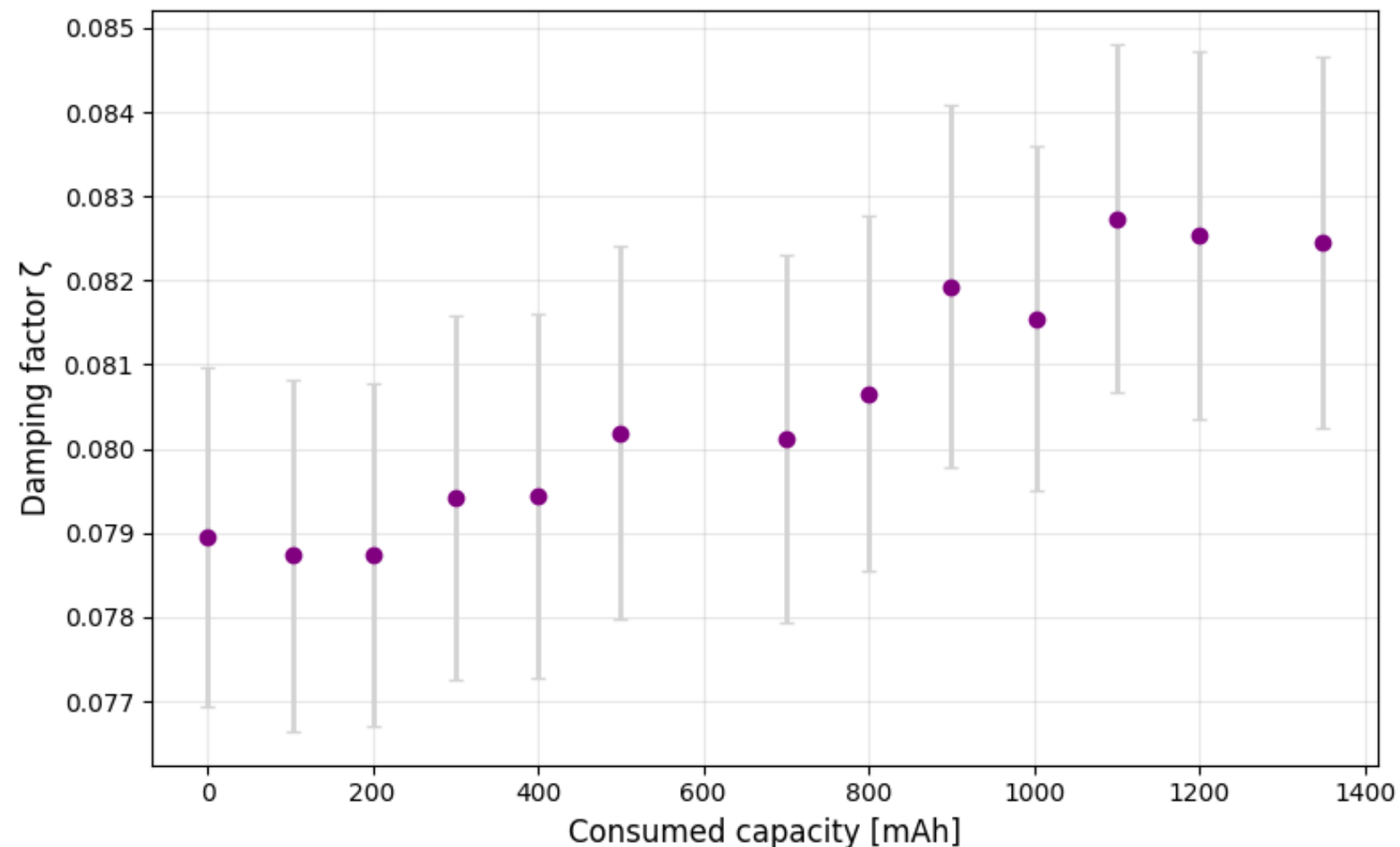
$$X(\omega) = \frac{F_0/m}{\sqrt{(\omega_0^2 - \omega^2)^2 + (2\zeta\omega_0\omega)^2}} \quad \zeta = \frac{c}{2\sqrt{mk}}$$



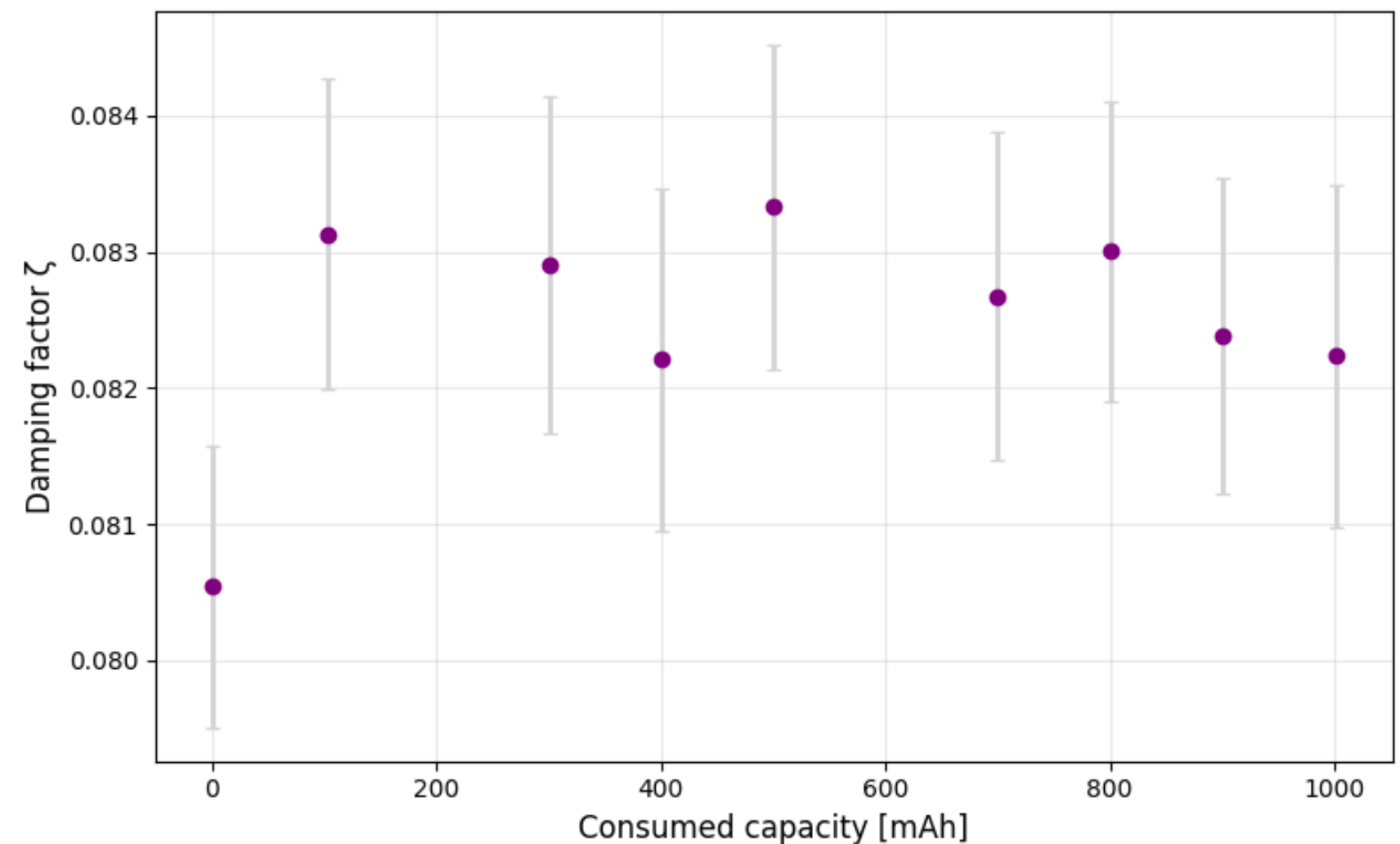
Fit to find ζ
the dampening factor for a battery

The piezo method – results

first try



second try



- Weak energy, opposite behaviour
- preconstraint change

The piezo method – analysis

There is a threshold of power :

For the rebound : $P = \frac{mgh}{\Delta t_{impact}} = \frac{0.023 \times 9.81 \times 0.22}{0.004} = 12\text{W}$

For the forced oscillator : $P \leq P_{max} = F\omega\delta \approx 1 \times 2\pi 500 \cdot 10^3 \times 100 \cdot 10^{-9} = 0.3\text{W}$



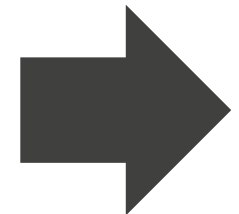
a hundred times too weak !!

The piezo method – analysis

What now ?

More powerful piezos

- ordered piezos capable of a displacement up to $\sim 30\mu\text{m}$
- and a force up to $\sim 8\text{N}$
- translates to a max power 1000 times greater

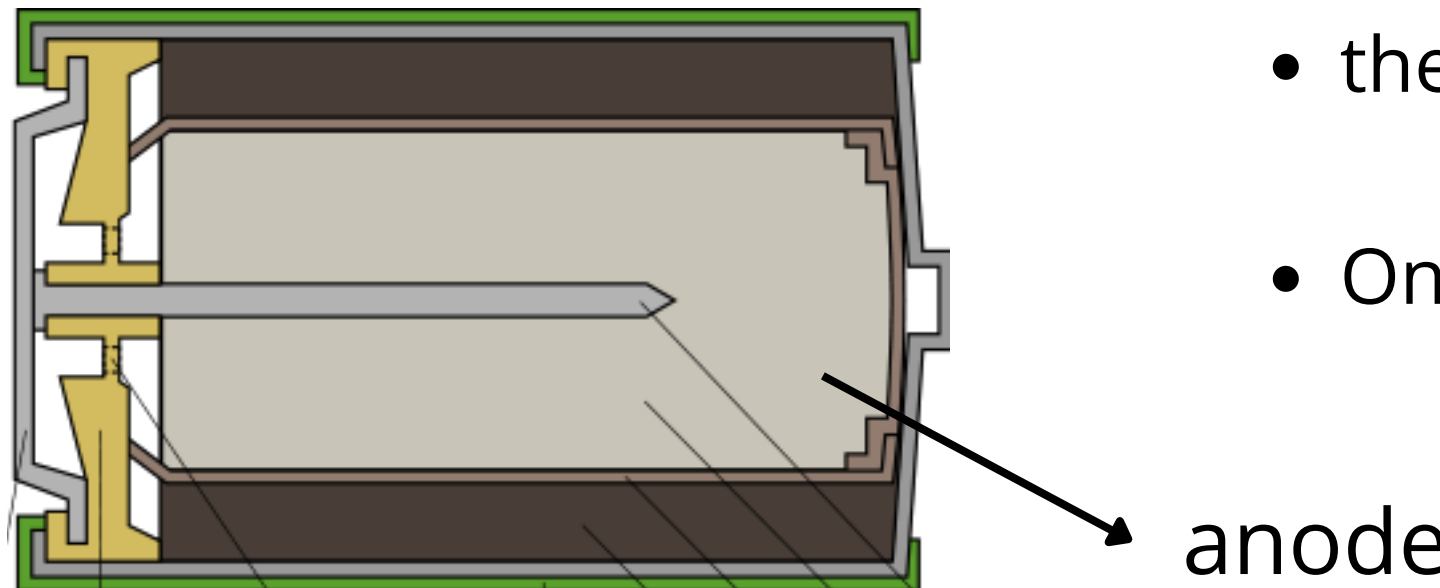


If the power was our limitation then we should be able to see something

The piezo method 2.0

Another method : time of flight

- Give an impulsion, or just a few cycles of a frequency
- determine the speed of sound by measuring the time it takes for the wave to come back
- Assuming the wave is low energy enough, we neglect the damping, and the amplitude of the returned wave is determined via the reflection coefficient : $R = \frac{Z' - Z}{Z' + Z}$
- the acoustic impedance is also given by $Z = \rho v$
- One can experimentally find the density ρ

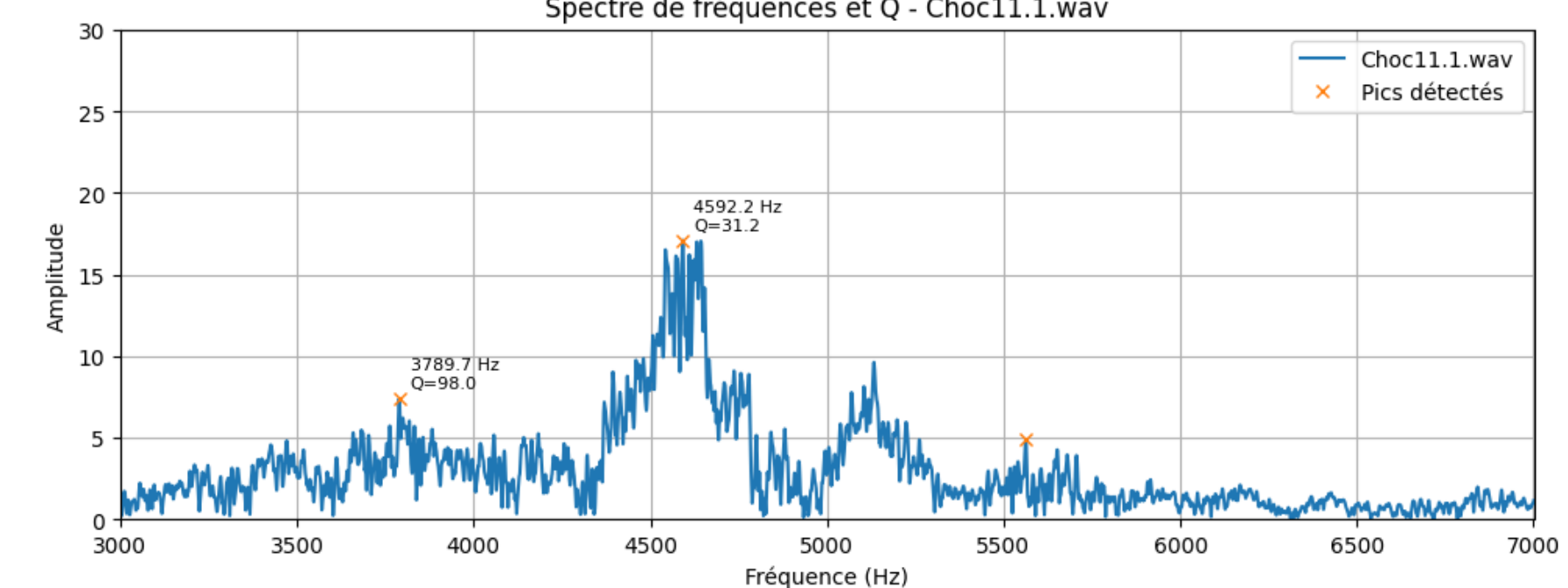
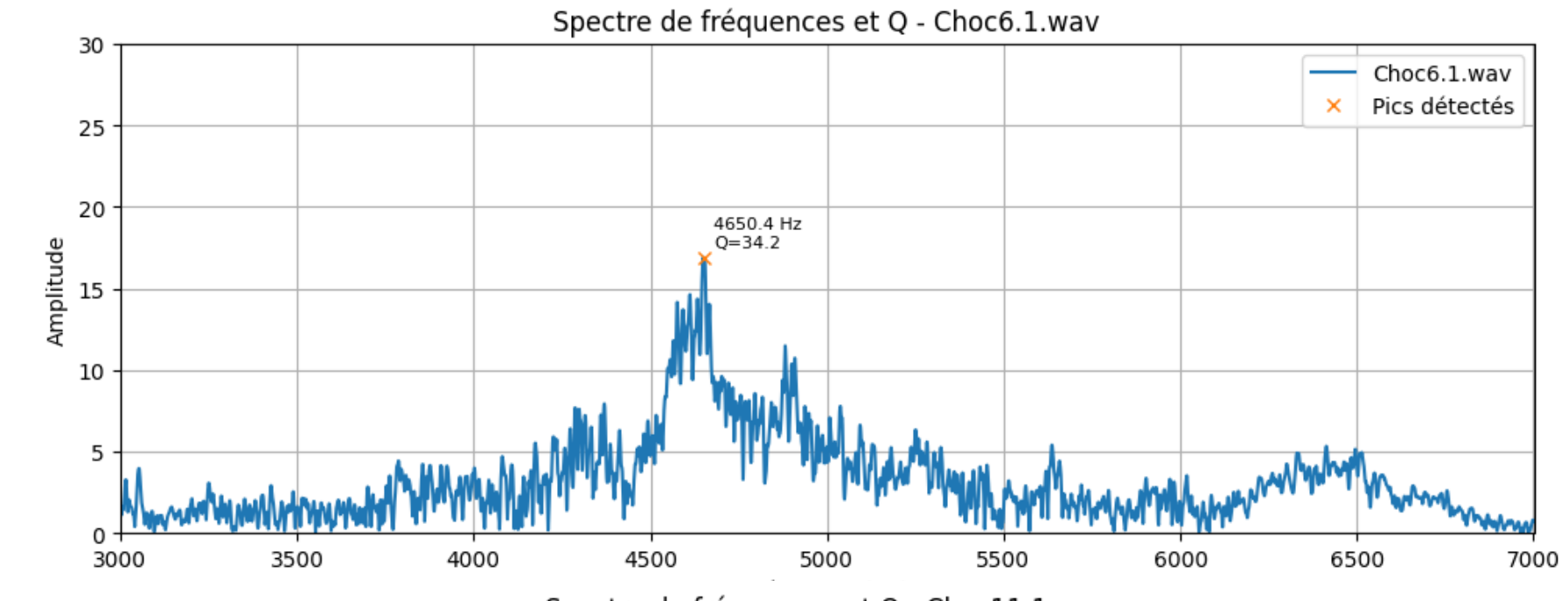
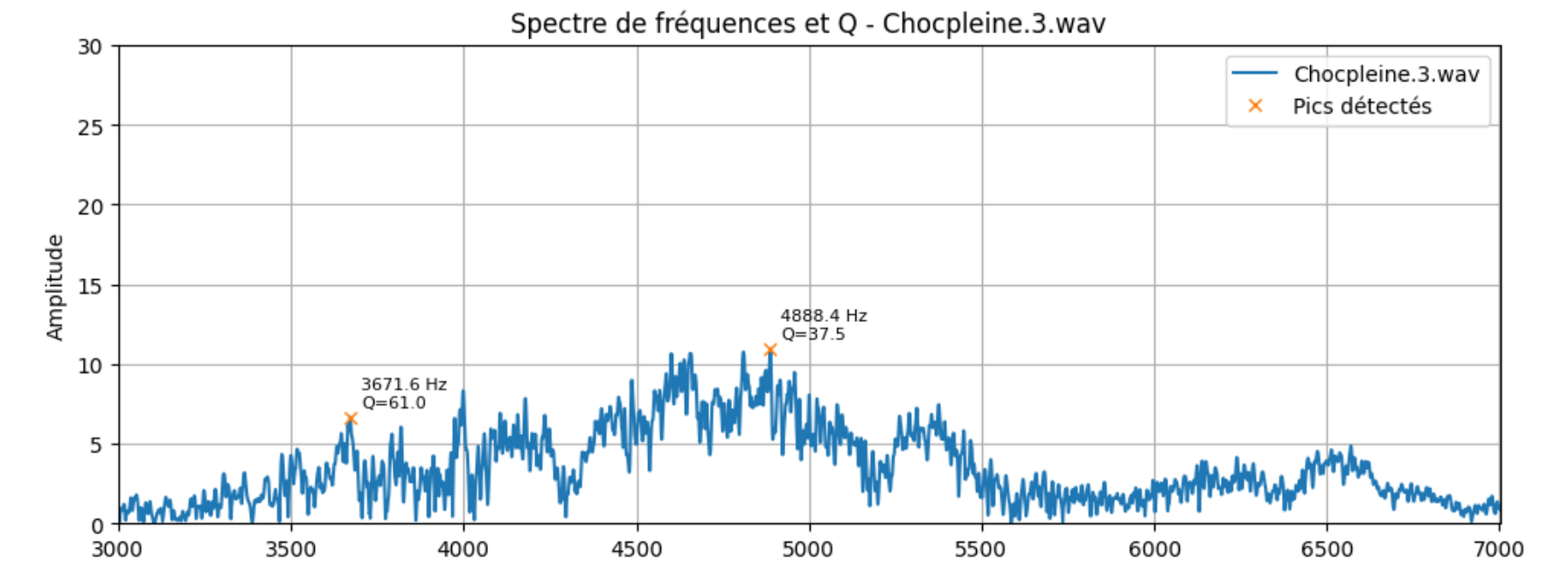


One can model directly via the known density change of the anode

Sound impact



- Increase of the quality factor
- Less damping = clear sound
- difficult to modelise what happens
- (but not been able to reproduce those results)



Other ideas



1)

- make it turn fast,
- cut the alimentation,
- and study the exponential decay of the angular momentum

2)

- Put an AC potential for the motor
- Observe how rapidly the movement is able to follow
- More powerful transfers
- Suspiciously low power power
- Peak to peak estimation (à revoir) :

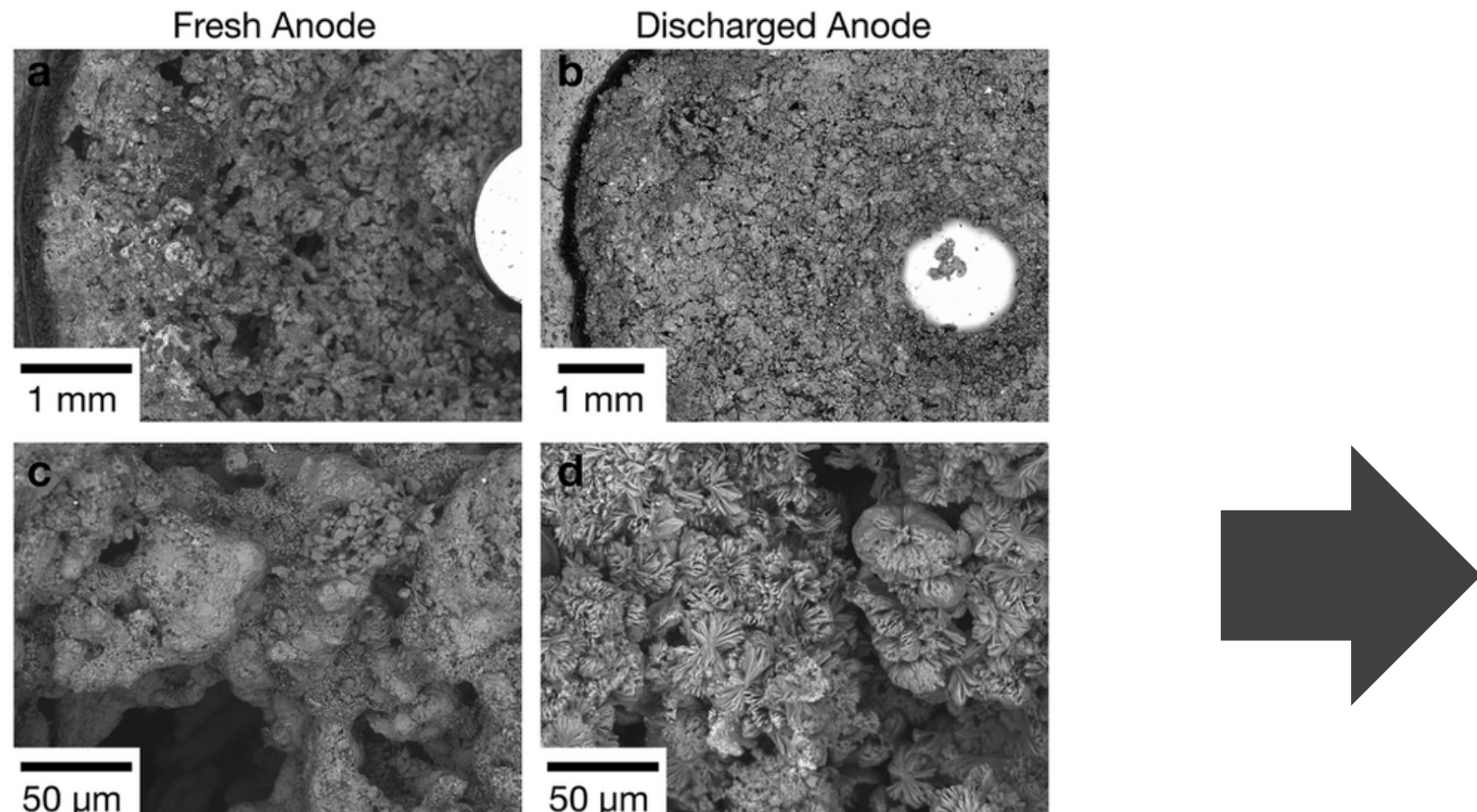
$$P = 10^{-8} \text{W}$$

No violent tenergy transfers → unlikely to observe something

Annexes

Specifications study's results :

2. Microscopic internal pictures (Post Mortem)



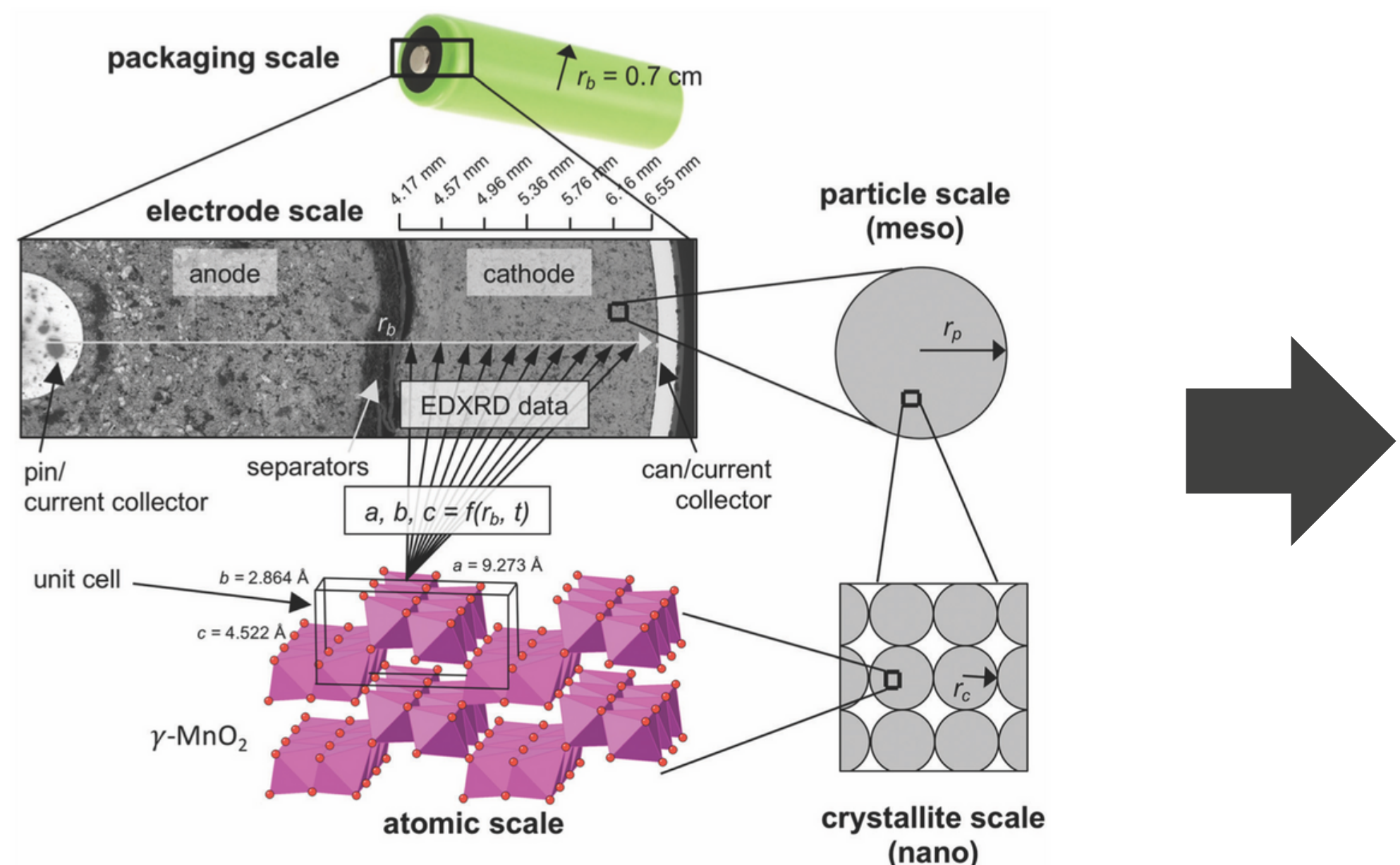
The anode densifies during the discharge. It is mostly composed of coagulated ZnO which create a rigid structure

Fig. 1 (a) SEM image of "fresh" cell, where the coarse zinc gel can be seen surrounding the current collector. (b) SEM image of the same cell after full discharge (2850 mA h passed), the anode now largely converted to ZnO. A more compact morphology is seen closest to the separator, with more granular morphology near the pin. (c) High mag. SEM image showing fresh Zn particles. (d) High mag. SEM image showing coagulated ZnO particles after full discharge.

Annexes

Specifications study's results :

3. Energy-dispersive X-ray diffraction



Analytical technique for characterizing materials *in situ*, by collecting diffraction patterns

Fig. 3 The scales involved in a porous cathode in which the active material is generally spherical particles, which in turn are agglomerates of spherical crystallites. EDXRD allows the atomic scale unit cell to be known as a function of location across the electrode scale.

Annexes

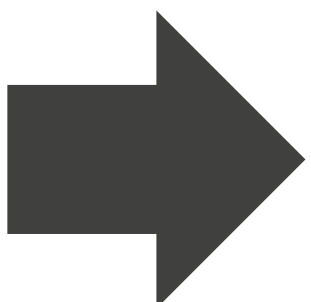
Specifications study's results :

4. Mechanical properties of material comparison

Table 3 Materials properties

Material	Density (g cm ⁻³) ²⁹	Bulk Modulus (GPa)
Zinc (Zn)	7.05	59 (ref. 30)
Zinc oxide (ZnO)	5.06	134 (ref. 31)
Ramsdellite (MnO ₂)	4.37	119 (ref. 32)
Groutite (MnOOH)	4.14	96 (ref. 33)

$$K = -V \frac{dP}{dV}$$



The bulk modulus K is a measure of a material's resistance to uniform compression.

Annexes

Discharge protocol

- Different states of charge were established by discharging the batteries at a constant current of 0.5A for controlled durations, thereby extracting well-defined amounts of capacity
- Total of 15 batteries were discharged in 100 mAh increments
- Maximum extractable capacity was slightly below 1400 mAh, which proved sufficient to observe and characterize the bouncing phenomenon



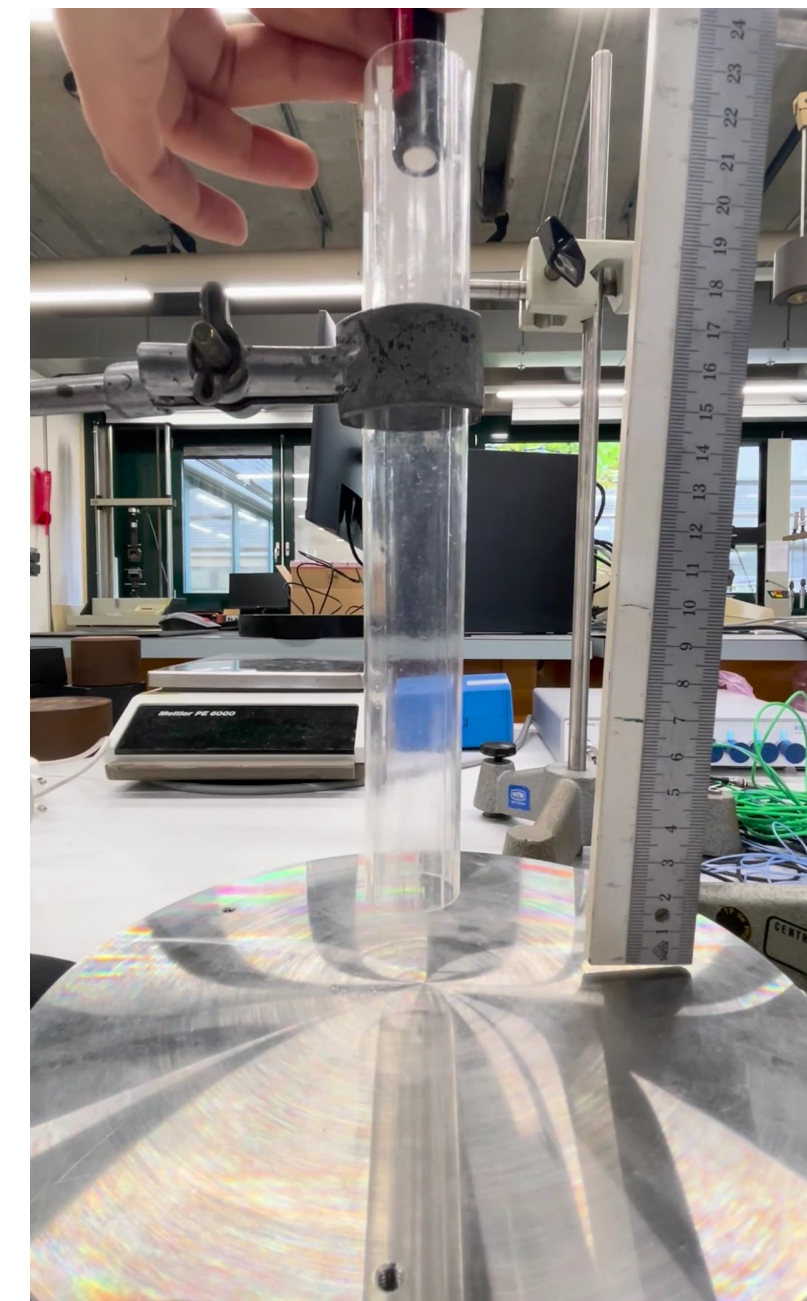
Absima charger CTC-1 Touch, used in discharger mode

Annexes

Bounce Videos



Full capacity



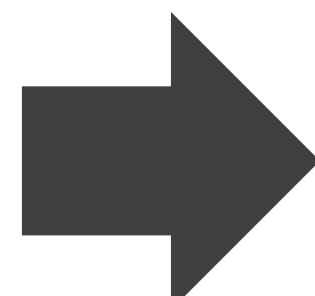
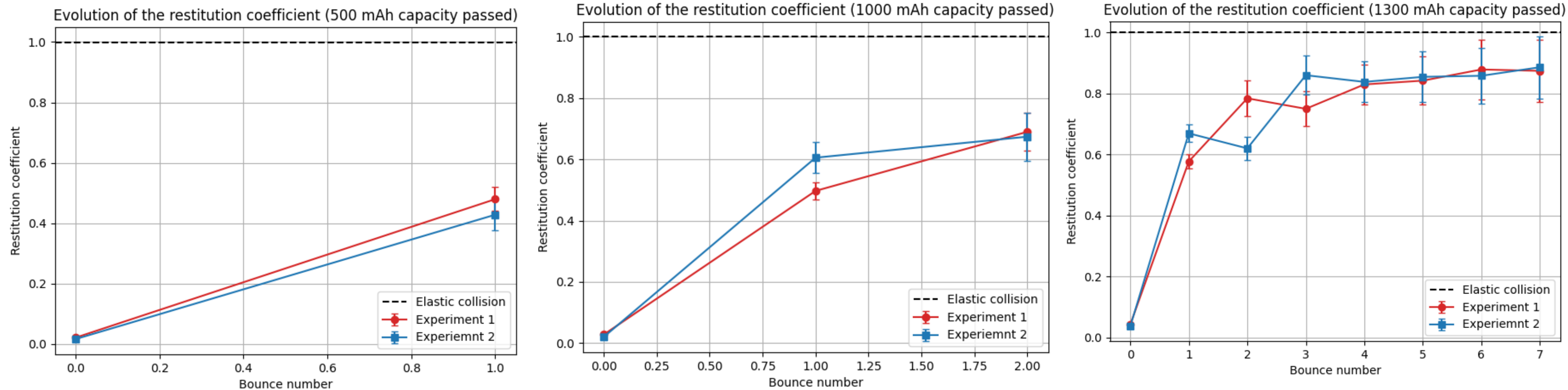
800 mAh passed capacity



1300 mAh passed capacity

Annexes

Evolution of the coefficient of restitution for different batteries

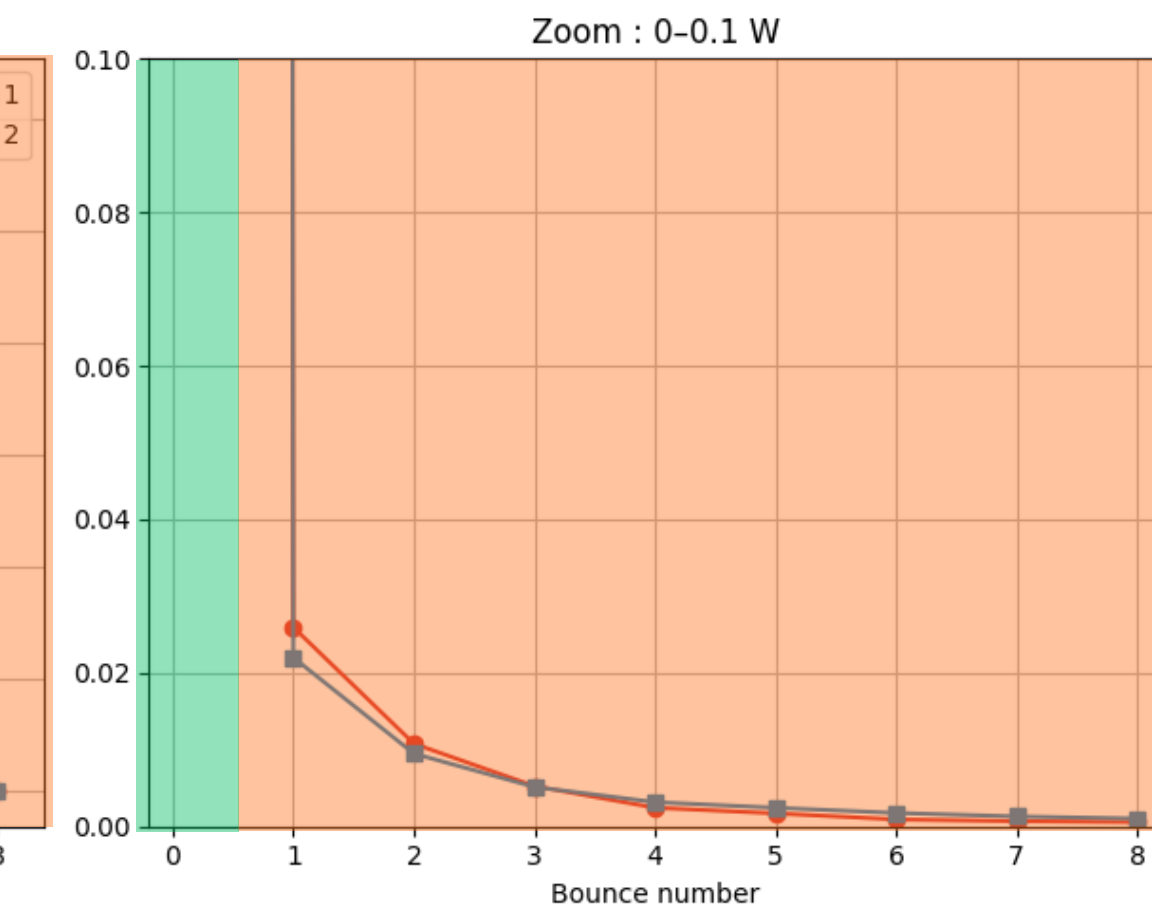
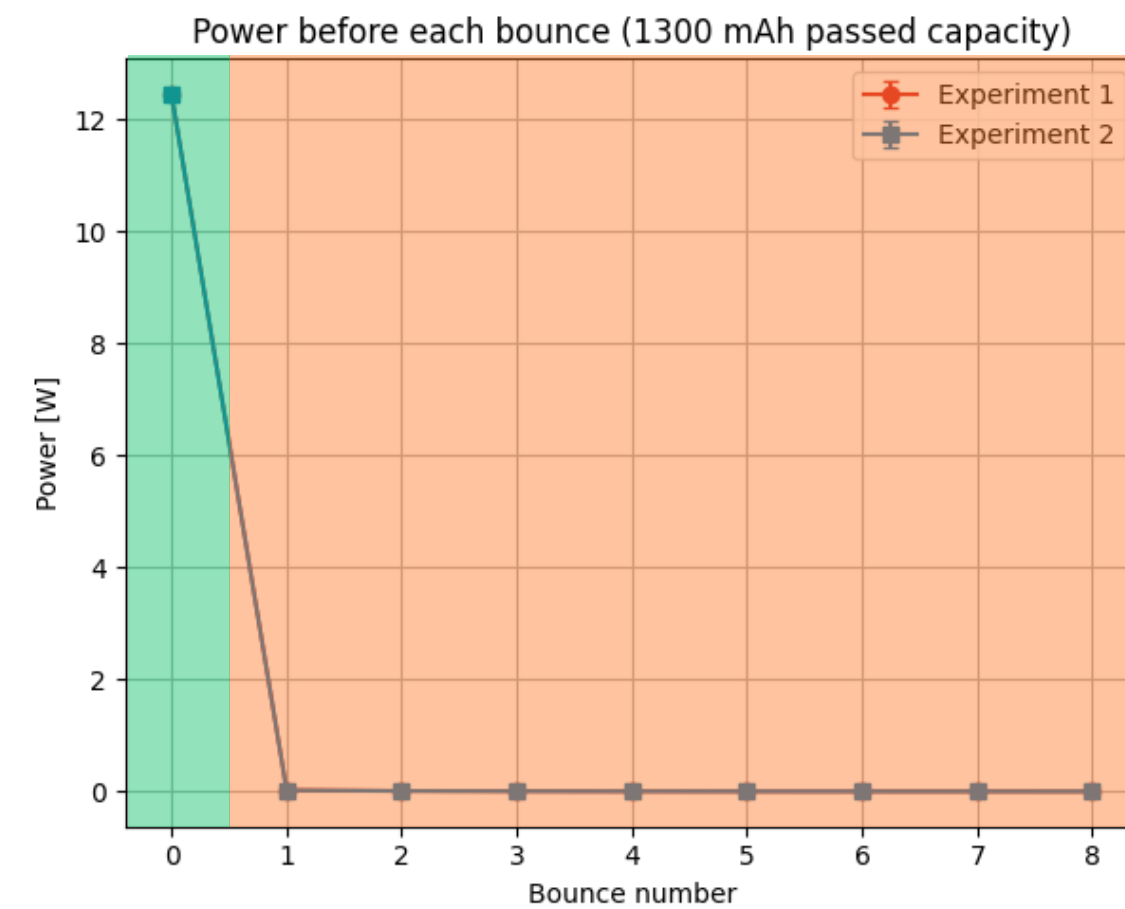


Increase of the coefficient of restitution measurable for batteries that underwent more than two bounces, suggesting a evolution of damping property as a function of the transmitted energy

Annexes

Energy range comparison

High Energy



Low Energy

